

Hydrothermal alteration of volcanic rocks hosting the Late Jurassic-Early Cretaceous San Nicolás VMS deposit, southern Zacatecas, Mexico

Luis F. Vassallo*, José Jorge Aranda-Gómez and José Gregorio Solorio-Munguía

Universidad Nacional Autónoma de México, Centro de Geociencias, UNAM Campus Juriquilla, Boulevard Juriquilla No. 3001, C.P. 76230, Juriquilla, Querétaro, Mexico.

* vassallo@unam.mx; skyzoloto@yandex.ru

ABSTRACT

San Nicolás is a Late Jurassic-Early Cretaceous, stratiform Zn-Cu-Ag-Au volcanogenic massive sulfide (VMS) deposit located in central Mexico, with a total resource of 99 Mt of ore grading 1.36 % Cu, 1.64 % Zn, 0.41 g/t Au and 24 g/t Ag. At San Nicolás mining district the ore deposits are related with submarine graben-horst structures produced by the opening of the Gulf of México. San Nicolás VMS deposit is at the right side of a graben structure, fed through a normal growing fault called "La Panza". The host-rock succession consists of a variably altered rhyolite lava dome in the hanging wall and a basalt-dacite-dominated volcano-sedimentary sequence in the footwall. The sulfide deposit and hosting volcanic sequence were metamorphosed under lower greenschist facies.

A laterally continuous footwall alteration zone extends beneath the entire district (~80 km²) and to a stratigraphic level at least 200 m below the several ore lenses. The bulk of this zone is occupied by feldspar-destructive, muscovite-biotite-chlorite-rich, mottled alteration facies with disseminated pyrite. The ore mineralization was controlled by a fault zone with intense quartz-pyrite alteration and represents the principal fluid pathway during mineralizing hydrothermal activity. Locally, quartz-K feldspar alteration facies occur on the edges of the system, whereas calcareous alteration and chlorite-pyrite alteration facies occur in the upper part of footwall volcanics, next to sulfide lenses. Porphyritic basalts, plus basaltic pillow lavas and volcanic breccias in the hanging wall are unaltered or weakly altered.

Carbonate alteration (formation of dolomite and/or ankerite) probably represents the initial phase of hydrothermal activity. This was followed by diffuse upwelling of acidic hydrothermal fluids causing dissolution of underlying limestones and destruction of primary feldspars, precipitation of pyrite, and formation of sericite, chlorite, and clay minerals. Subsequently, intense quartz-pyrite alteration was directly associated with mineralization.

The San Nicolás footwall alteration zone shows systematic geochemical changes with increasing proximity to the ore bodies. These include Na depletion and elevated Mg, S, Al (Al=100*[MgO+K₂O]/[MgO+K₂O+Na₂O+CaO]), CCPI(CCPI=100*[MgO+FeO]/[MgO+FeO+Na₂O+K₂O]), as well as Mo, Bi, and As. These geochemical features can be used in exploration for massive sulfide deposits as

guides to ore, at the district scale, and in discrimination of prospective hydrothermal from unprospective diagenetic alteration systems at the regional scale.

Key words: Mexico; alteration; Jurassic volcanics; VMS.

RESUMEN

San Nicolás es un depósito estratiforme de sulfuros masivos vulcanogénicos de edad Jurásico Superior-Cretácico Inferior con Zn-Cu-Ag-Au, localizado en la parte central de México, con reservas de 99 millones de toneladas con leyes de 1.36 % de Cu, 1.64 % de Zn, 0.41 g/t Au y 24 g/t Ag. En el distrito minero de San Nicolás los depósitos minerales están relacionados con estructuras submarinas de horst-graben producidos por la apertura del Golfo de México: el depósito de San Nicolás se ubica en la parte derecha de una estructura de graben, alimentado por medio de una falla normal de crecimiento llamada "La Panza".

La sucesión de rocas encajonantes variablemente alteradas consiste de un domo riolítico en la parte superior (bloque de techo) y una secuencia volcánico-sedimentaria predominantemente de basaltos y dacitas en la parte inferior (bloque del piso). El depósito de sulfuros y sus rocas encajonantes fueron metamorfizadas en grado de fácies de esquistos verdes.

Lateralmente, en el bloque del piso, se extiende una zona de alteración en todo el distrito (~80 km²) y a un nivel estratigráfico hacia abajo de los mantos de hasta 200 m. La mayor parte de esta zona es ocupada por facies de destrucción de feldespatos, muscovita-biotita-clorita y alteración puntuada con diseminación de pirita. La zona de la falla presenta una alteración intensa de cuarzo-pirita y representa el camino principal de los fluidos durante la actividad hidrotermal mineralizante. Localmente hay facies de cuarzo-feldespato potásico en los bordes del sistema, y la alteración calcárea y las facies de clorita-pirita se presentan en la parte superior de las rocas volcánicas del bloque del piso, al lado de los mantos de sulfuros. Basaltos porfiríticos, lavas almohadilladas y brechas volcánicas en el bloque de techo están inalterados o levemente alterados.

La alteración calcárea (formación de dolomita y/o ankerita) probablemente representa la fase inicial de la actividad hidrotermal. Lo anterior fue seguido por una difusión ascendente de fluidos ácidos lo cual causó la disolución de las calizas subyacentes de formaciones conocidas y la destrucción de los feldespatos primarios, precipitación de pirita y

formación de sericita, clorita y de minerales arcillosos. Posteriormente, una fuerte alteración cuarzo-pirita se relaciona con la mineralización.

La zona alterada del bloque del piso de San Nicolás muestra cambios geoquímicos sistemáticos con una variación de la distancia a la proximidad a los cuerpos minerales. Esto incluye una disminución de Na y elevación de Mg, S, Al, ($AI=100*[\text{MgO}+\text{K}_2\text{O}]/[\text{MgO}+\text{K}_2\text{O}+\text{Na}_2\text{O}+\text{CaO}]$), $CCPI(CCPI=100*[\text{MgO}+\text{FeO}]/[\text{MgO}+\text{FeO}+\text{Na}_2\text{O}+\text{K}_2\text{O}])$, Mo, Bi y As. Estas características geoquímicas pueden ser usadas en la exploración por sulfuros masivos (MVS) como guías hacia las menas, en la escala de distrito y como vector discriminador de prospectos hidrotermales de sistemas diagenéticos alterados no prospectivos a escala regional.

Palabras clave: México; alteración; rocas volcánicos del Jurásico; MVS.

INTRODUCTION

The western North American Cordillera hosts important gold-bearing quartz veins, silver-bearing quartz veins, volcanogenic massive sulfide (VMS) deposits and Zn-Cu-Pb-Ag skarns systems including the silver belt of central Mexico, the Mother Lode of southern California, and counterparts in British Columbia and southeastern Alaska, to the Klondike district in central Yukon. All these veins, VMS and skarns systems are structurally controlled by major fault zones or weakness zones, which are often reactivated terrane-bounding sutures that formed in orogens built during accretion and subduction of terranes along the continental margin of North America, and in México along the faults (Figure 1) related to the opening of the Gulf of México, (de Cserna, 1976a, Pindell, 1985, Vélez, 1990, Vassallo, 2003, Vassallo *et al.*, 2004, Piercy, 2011, Pindell *et al.*, 2012). Mineralization ages span mid-Jurassic to early Tertiary (Vassallo *et al.*, 2000, 2004). The VMS

are related with high-temperature magmatism within well-defined thermal corridors, as those described by Piercy (2011), associated with extensional geodynamic settings in volcanogenic environments, Sillitoe, (1982). VMS deposits are determined by tectonic regime change, evolution of the continental lithosphere composition, and irreversible transformations occurring in the Earth's atmosphere, hydrosphere, and biosphere, Dergachev and Eremin, (2008).

Hydrothermal alteration assemblages of VMS have been investigated from mineralogical, textural, petrophysical, and chemical perspectives (e.g., Starostin, 1979, 1984; Franklin *et al.*, 1981; Starostin and Dergachev, 1982; Lesher *et al.*, 1986; Eastoe *et al.*, 1987; Morton and Franklin, 1987; Gemmell and Large, 1992; Large, 1992; Huston, 1993; Khin *et al.*, 1996; Paulick *et al.*, 2001; Schardt *et al.*, 2001; Solomon and Gaspar, 2001; Starostin *et al.*, 2002). Much of this research has contributed to the knowledge of composition, mineralogical and chemical zonation of footwall alteration systems below massive sulfide systems, which are the sites of intense fluid-rock interaction in the upflow or vent zone below the sea floor. Due to metamorphism, tectonic deformation, and lack of access to alteration pipes, few studies have focused on stringer zones of VMS and their alteration assemblages (Lydon, 1988).

San Nicolás is a Late Jurassic-Early Cretaceous, (Danielson, 2000, Iriondo *et al.* 2003, Mortensen *et al.* 2008), stratiform, polymetallic massive sulfide deposit hosted within a felsic-basic lava-dominated sequence in southern Zacatecas, Mexico. The deposit has a total mineral resource of 99 Mt with 1.36 % Cu, 1.64 % Zn, 0.41 g/t Au and 24 g/t Ag, (Johnson *et al.*, 2000). The San Nicolás ore consists of variable proportions of pyrite, sphalerite, galena and chalcopyrite, with gangue chlorite, tremolite, calcite, dolomite, barite, magnetite and quartz. Massive and semi-massive sulfides occur in a single horizon at the stratigraphic contact between rhyolite domes in the hanging-wall and a volcano-sedimentary sequence dominated by mafic lavas

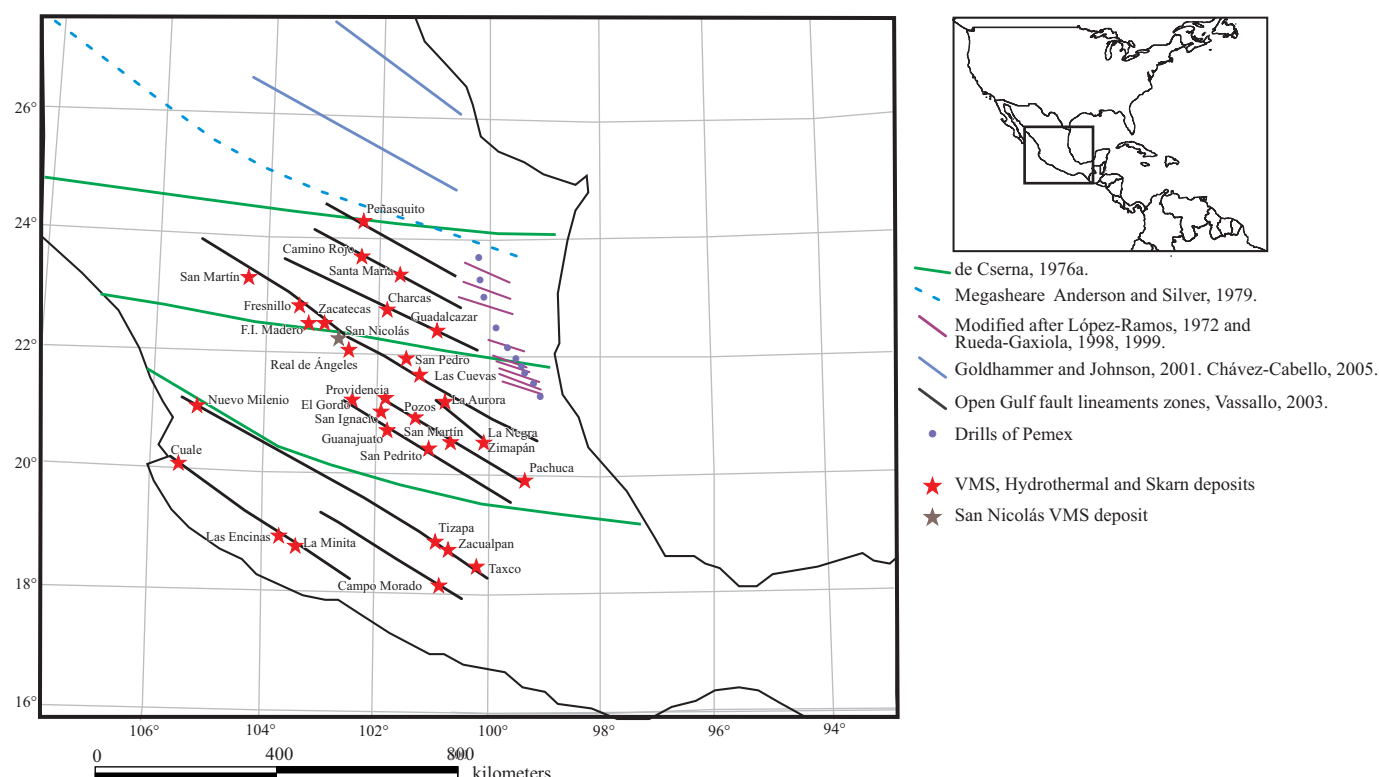


Figure 1. Ore deposits of Central Mexico. With Jurassic-Cretaceous faults modified after De Cserna (1976a), Vélez (1990), and others.

in the footwall. This rhyolite horizon is referred to the “San Nicolás favorable unit” in this paper. Below the San Nicolás deposit there is a texturally, mineralogically and geochemically diverse strata-bound alteration zone that extends across the controlling mineralization fault zone into the footwall at least 200 m down, with gradational contacts to the surrounding unaltered or weakly altered volcanic rocks.

It has been recognized (Smirnov, 1944, 1963, 1968, 1976; Yakovlev, 1959) that footwall alteration zones associated with volcanic massive sulfide (VMS) deposits may have a stratabound geometry or a discordant, pipelike shape. A comparative study of Australian VMS (Large, 1992) and VMS in Russia and Kazakhstan (Yakovlev, 1959; Smirnov, 1976; Smirnov and Gorzhevskii, 1978; Starostin, 1984), showed that most deposits have stratabound and semiconformable footwall alteration zones. Well-defined, pipelike alteration zones, such as those associated with Precambrian deposits of Noranda-Canada, (Sangster, 1972; Barrett and MacLean, 1994; Shriver and MacLean, 1993), Paleozoic deposits of Rudnii Altai (Yakovlev, 1959; Smirnov, 1976; Smirnov and Gorzhevskii, 1978) and Tertiary Kuroko deposits, (Ohmoto and Skinner, 1983; Shikazono *et al.*, 2008), are common worldwide.

The study of stratabound alteration zones is relevant for base metal exploration and for research in rock-water interaction processes. Because of their large extent below the deposit, stratabound alteration zones provide better exploration criteria than the spatially confined alteration pipes. However, in contrast to pipelike alteration zones, stratabound footwall alteration zones typically lack clear boundaries of mineralogical zoning that increases the difficulty for massive sulfide exploration.

Careful examination of geological, petrographical, and geochemical data is required to discriminate the large-scale alteration zones generated by general mineralizing hydrothermal activity from alteration related to syn-volcanic seafloor alteration processes.

This paper provides a regional geological appraisal and a detailed description of alteration observed at San Nicolás ore deposit, including textural, mineralogical and geochemical characteristics. Several geochemical features like CCPI, AI, Na₂O, show systematic variations with increased proximity to the massive stratabound sulfide deposits.

REGIONAL GEOLOGY

The San Nicolás deposit is located in a NW-SE-trending belt of deformed Jurassic-Cretaceous marine sedimentary and volcanic rocks defined in this paper as the Chilitos Group in the central part of Mexico (Figure 2). The lower unit of this group was defined first by de Cserna (1976a) as Chilitos Formation. Discontinuous outcrops over a distance of more than 300 km (Zacatecas to Guanajuato) expose a grossly conformable stratigraphic succession, up to 1.5 km thick, with gentle folding and NW 45° axis orientation. The group was intruded by Jurassic to early Tertiary plutons (El Saucito, Peñón Blanco and Comanja type plutons). Mesozoic rocks are for the most part covered by the Tertiary rhyolitic La Bufa Formation and others minor volcanics by semiconsolidated alluvium.

The Chilitos Group was divided into three conformable formations (Vassallo, 2012). At the base is the Arroyo Chilitos Formation, (de Cserna, 1976b), which consists of dominantly basaltic to andesitic sills and lavas, similar to those described at Guanajuato, (Vassallo, 1988a, 1988b; Vassallo *et al.*, 1989; Freydier *et al.*, 1997, 2000, Vassallo and Reyes-Salas, 2007, Aranda-Gómez *et al.*, 2012).

The overlying San Nicolás Formation mainly consists of rhyolitic lavas, synvolcanic intrusions and volcaniclastic rocks. The crystallization age of a rhyolite sample is given by the total range of 206Pb/238U

ages for three concordant analyses (146.5±2.2 Ma) dated using U-Pb zircon methods (Mortensen *et al.*, 2008). The upper La Virgen Formation comprises lithic sandstone and graywacke with some basaltic lava (Table 1) with a hornblende age of 117.94 Ma (Iriondo *et al.*, 2003), synvolcanic intrusions, and various volcaniclastic and sedimentary rocks. Geochemical data suggests that the volcanic rocks of the Chilitos Group were emplaced in an active continental margin (Schandl and Gorton, 2002). The Chilitos Group was wide folded and took a tilted position during regional normal faulting in the Aptian. The area probably represents the northeastern part of a large NW-SE trending overthrust structure, and in some places the Chilitos Group overthrusts the Lower Cretaceous limestone of the Proaño Group (Trejo, 2001), as seen in the Town of Fresnillo (de Cserna, 1976b). The regional metamorphic grade increases from sub-greenschist in the eastern part to greenschist in the western part of the Zacatecas state (Vassallo and Solorio-Munguia, 2005).

In early Tertiary, the Saucito and Peñón Blanco plutons were emplaced (Aranda *et al.*, 2007), which postdates the end of Laramide deformation (Aranda *et al.*, 2007; Vassallo *et al.*, 2008). Its porphyritic texture, with beta quartz pseudomorphs and euhedral sanidine phenocrysts suggests a shallow subvolcanic intrusion. The absence of penetrative fabrics associated with folding and/or shearing indicates a post-tectonic emplacement. A ⁴⁰Ar/³⁹Ar age of 49.5 Ma constrains the end of Laramide deformation in this area (Aranda *et al.*, 2007).

Tertiary rhyolitic rocks from 32 to 27 Ma cover the mining district. Samples MC-14, 15, 20, 33 and P5-95 (Table 1) provide several ages for the known volcanic episode at Pinos, Zacatecas, 20 km east of San Nicolás, (Aranda *et al.*, 2007).

A later phase of Miocene extensional faulting is associated with the NE-SW faults structures that formed large grabens and cut the VMS deposits and Eocene clastic units (Figure 3).

GEOLOGICAL SETTING OF THE SAN NICOLÁS ORE DEPOSIT

San Nicolás ore deposit is the largest known VMS deposit in central Mexico. The San Nicolás mining district contains several stratiform, mound or lense-shape orebodies, which extend over an area of more than 500 km², at the middle of the Chilitos Group. The San Nicolás deposit and its host-rock succession are examined here in 5 drill core-based cross sections through the deposit (Figures 3 and 4).

A model for the paleofacies architecture of the host-rock succession is reconstructed based on structural-volcanic analysis. The San Nicolás deposit formed on a paleochannel or graben produced by Jurassic-Cretaceous growing longevity faults, that act as feeders of marine bimodal-felsic volcanic rocks as Kuroko type deposits of Piercy, (2011), one of them La Panza fault is the principal control of the mineralization (Figures 4, 5). This geologic setting is analogous to the environment of the modern PACMANUS hydrothermal field, Manus Basin, Papua New Guinea, (Binns and Scott, 1993), and others described by Schulz, (2012). Lydon, (2010) also recognized the important role that have the synsedimentary faulting and the growing longevity faults that control the mineralization also in Sedex (VMS variant) deposits at B.C. Canada.

The footwall alteration zone at San Nicolás is laterally continuous along the strike extent of the deposit and extends for at least 200 m into the hosting volcanic rocks. Nevertheless, Larson (1984) found in the footwall andesitic rocks at Bruce VMS deposit, Arizona, that the alteration zone extends for at least 400 m away from the ore lenses.

Contacts with the surrounding unaltered basalts are gradational. Moderately altered rhyolite represents the bulk of the footwall altera-

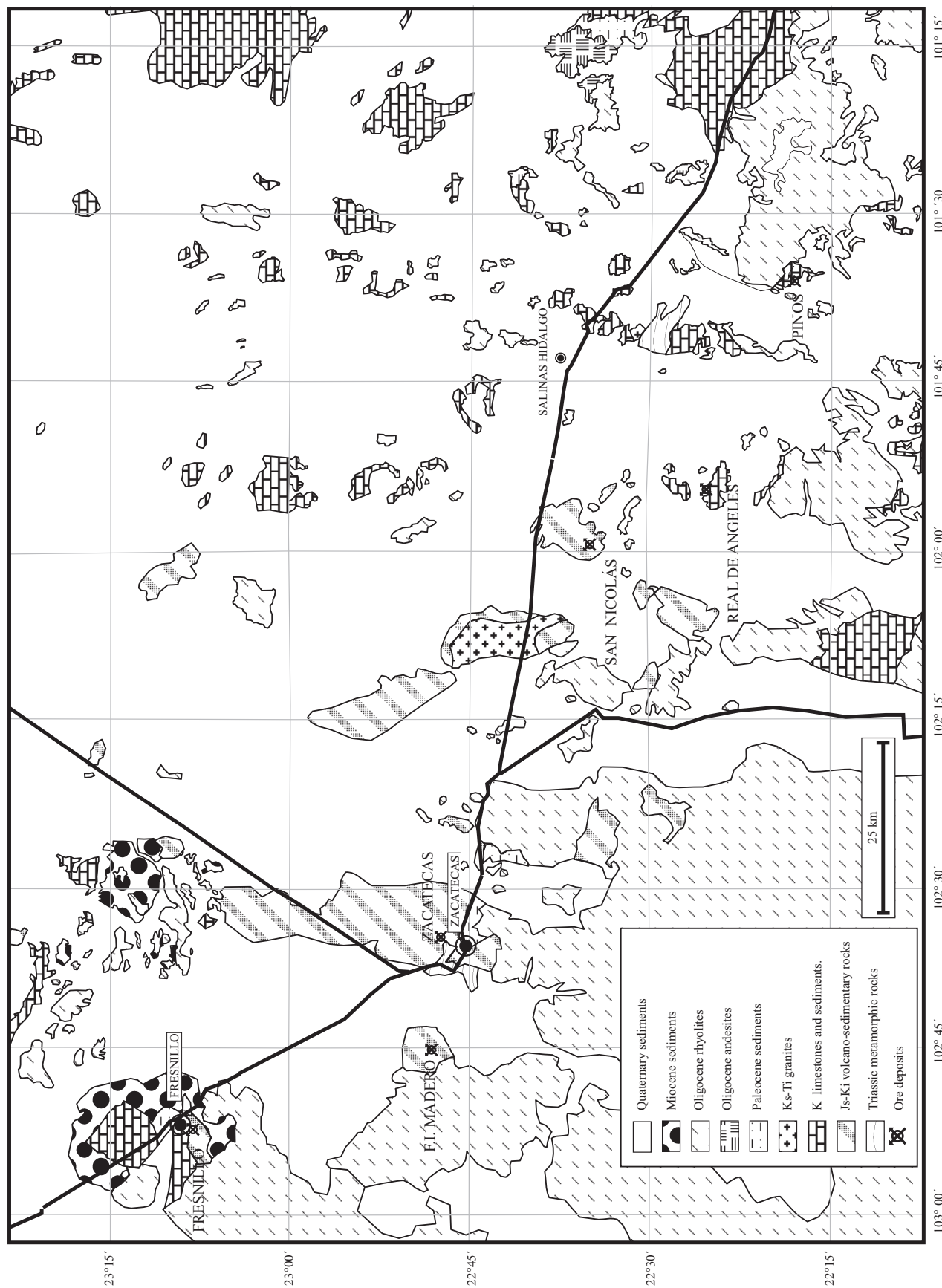


Figure 2. Regional geology of San Nicolás area.

Table 1. Age Determinations of rocks. Modified after Aranda-Gómez *et al.* (2007).

Sample	Material	%K	$^{40}\text{Ar}^*$	%Ar*	Age (Ma)	2s	
MC-14	San	6.205	7.677	81	32.32	3.1	
		6.191	7.710	72			
			8.404	78			
			7.620	87			
P5-95	wr	5.070	0.583	94.8	30	3.0	
		0.585	0.585	95.1			
MC-15	San	8.660	9.450	91	28.67	1.80	
		8.446	9.783	88			
			9.270	81			
			9.904	88			
MC-33	San	4.864	6.414	76	28.7	1.4	
		4.682	6.225	64			
			5.456	78			
MC-20	San	6.185	6.567	77	27.28	1.2	
		6.265	6.660	72			
			6.677	66			
			6.691	68			
$^{40}\text{Ar}/^{39}\text{Ar}$ Data		Age method		Age (Ma)			
MC-14		m.w. plateau		30.69			
MC-35		m.w. plateau		49.51			
PAR-2*		plateau age		117.94			

Notes for K-Ar data: $^{40}\text{Ar}^*$ ($\times 10^{-6}$ sec/g), %Ar* = percent radiogenic argon; K-Ar analyses by Fred McDowell and Teledyne Isotopes (sample P5-95).

Notes for $^{40}\text{Ar}/^{39}\text{Ar}$ data: Decay constants: $1b=4.963 \times 10^{-10}/\text{year}$; $1e+e=0.581 \times 10^{-10}/\text{year}$; $40\text{K}/\text{K}=1.167 \times 10^{-4}$; WR=whole rock, Mus=muscovite, San=sanidine; $^{40}\text{Ar}/^{39}\text{Ar}$ analyses were done at Queen's University; Dates (integrated/plateau) and J-values for the intralaboratory standard; *Iriondo (2003)-USGS ofr-03-020.

tion zone and shows diverse textural, mineralogical and geochemical features, which are described below. Minor zones of intense alteration cut across the footwall alteration zone and extend up to the massive sulfide bodies (Figures 4, 5).

The San Nicolás deposit favorable host strata is up to 300 m thick lithologically diverse unit. It includes coarse, “quartz-eye” bearing volcaniclastic rocks, coarse porphyritic “quartz-eye” intrusions and a few rhyolite breccias. This volcanic succession includes massive to semimassive sulfide and massive to semi-massive barite orebodies.

The hanging wall of the normal fault consists of altered to weakly altered rocks, including volcaniclastic rocks and graywackes with some basaltic lavas overlying the San Nicolás Formation of porphyritic rhyolite. Volcaniclastic sedimentary rocks consist mostly of dacitic lithic clasts and some lithoclasts of basaltic lava.

Previous studies of the San Nicolás deposit have proposed that the orebody is syngenetic and massive sulfides were deposited onto the sea floor from dense saline solutions (Johnson *et al.*, 2000), and may have partially formed by sub-seafloor replacement of intensely altered rhyolite rocks. The arrangement of massive pyrite lenses in the San Nicolás unit, the distribution of barite, and variations in metal ratios of the massive sulfides along strike of the deposit indicate that mineralization occurred in 10 hydrothermal district fields (Figure 3). Parts of ore lenses with high Cu ratios ($\text{Cu}/(\text{Cu} + \text{Zn})$), low Zn ratios ($\text{Zn}/(\text{Zn} + \text{Pb})$) and basal zones of massive pyrite-chalcopyrite are interpreted as discharge sites of hot, metal-rich fluids, whereas massive

barite with disseminated sulfides represent peripheral, low-temperature zones of the hydrothermal system (Huston and Large, 1987).

The structural geology of the San Nicolás area was examined in detail by Johnson *et al.* (2000) and Vassallo (2003). Two generations of faults have been recognized. A NW-trending pattern of faults of Jurassic-Cretaceous age cut the footwall rhyolite rocks into an apparent hanging wall position (Figure 3). NW trending faults structures have been recognized at San Nicolás, for example the so called La Panza Jurassic-Cretaceous growing fault, (Figures 5, and 6) after Johnson *et al.*, (2000). The San Nicolás mining district is cut by a second NE-striking group of normal faults (Miocene Basin and Range structures of Vassallo, 2003; Figure 3).

ALTERATION FACIES AND GEOMETRY OF THE ALTERATION ZONE AT SAN NICOLÁS

Alteration at the San Nicolás deposit is mineralogically and texturally diverse and several alteration facies have been defined here on the basis of dominant mineral assemblages and alteration intensity with variable proportions of quartz, muscovite, chlorite, epidote, tremolite, calcite, K-feldspar, and pyrite, (Figures 6, 7). Alteration facies is a strictly descriptive term as proposed by Riverin and Hodgson (1980), and Vassallo (2003). In this paper alteration facies refers to rocks with modification of pristine characteristic mineralogical, petrographical, chemical and textural features.

There are 6 alteration facies from weak to intense degree (Figure 8):

1. *Weak alteration* is patchy or vein controlled and includes two different facies: Weak chlorite-sericite (weak chl-ser) alteration (Figure 7), and chlorite-pyrite-sericite (chl-py-ser) alteration (Figure 7).

Both facies are generally not texturally destructive. These alteration facies are particularly common in hanging-wall volcanic rocks. No clear systematic variations in the abundance or relative proportions of weak alteration facies have been observed with regard to the proximity to the massive sulfides (Vassallo, 2003). Phyllosilicate alteration is particularly prominent in the groundmass of volcaniclastic rocks in the hanging wall block, which likely were rich in fine-grained, glassy volcanic fragments and/or fine grain sedimentary clay minerals. Hence, it is inferred that these alteration facies reflect background alteration processes related to mineralizing hydrothermal circulation.

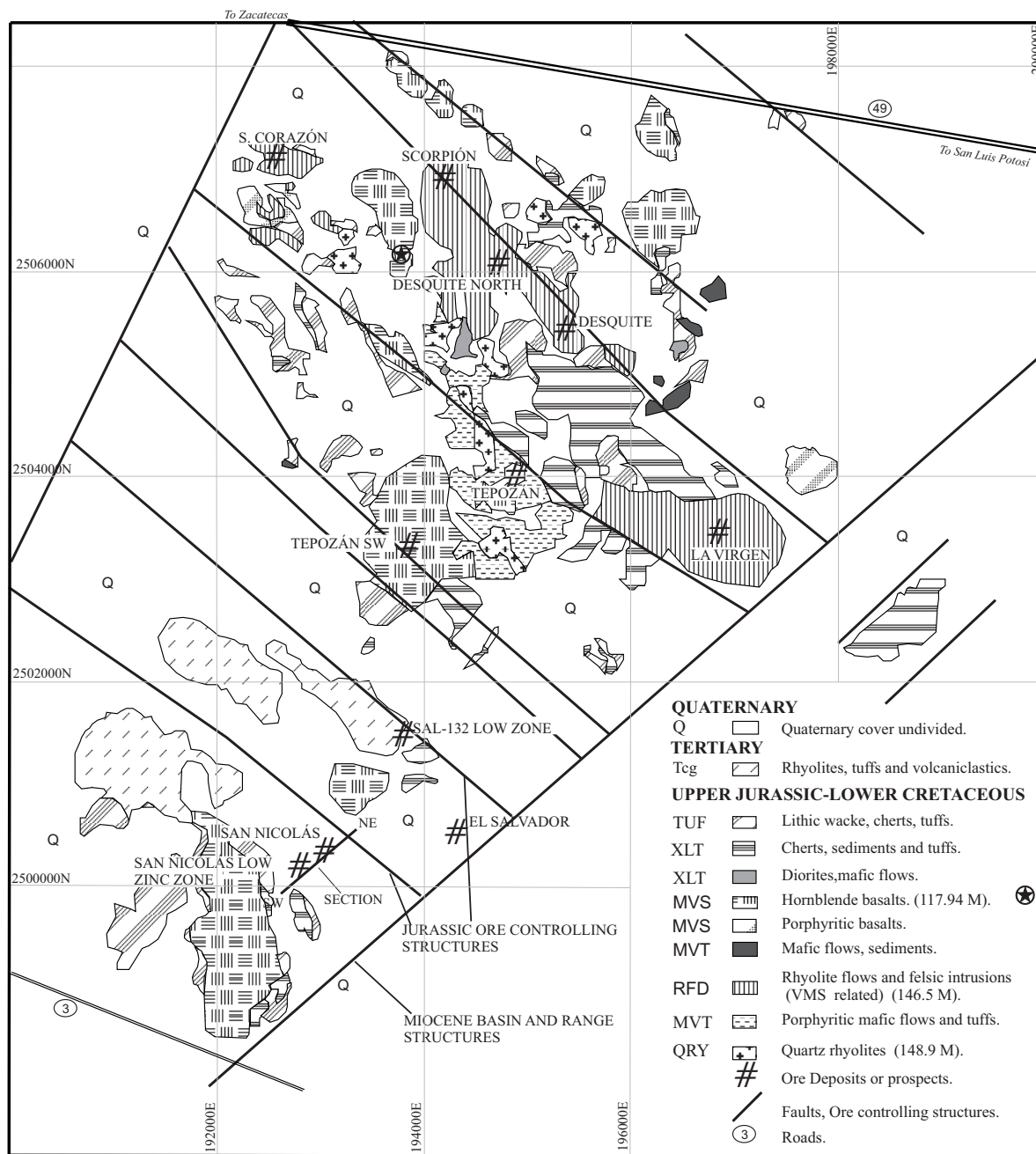
2. *Moderate to intense alteration* is confined to the footwall below the massive sulfides. Representative cross sections through San Nicolás deposit (Figures 5, 7) illustrate the arrangement of alteration facies. The footwall alteration zone consists predominately of:

3. *Feldspar-destructive, muscovite-chlorite-biotite-rich mottled (strong chl-py-ser-K-feldspar) alteration facies* (Figure 7) with minor disseminated pyrite (3 vol %). This alteration facies is characterized by substantial variations in the relative proportions of muscovite, chlorite, biotite and quartz, in hand specimen scale, producing textures which superficially resembling those of volcaniclastic rocks.

Such fabrics, which are related to one domain and/or multiphase alteration processes, are common in footwall alteration zones below VMS deposits and have frequently led to the misinterpretation of altered felsic lavas as primary pyroclastic rocks (Allen, 1988). Criteria for the discrimination of genuine clastic and apparent clastic textures at San Nicolás are presented in Vassallo and Solorio-Munguía (2005).

4. *The quartz-K-feldspar (intense qtz-py-ser) alteration facies* (Figure 7) occurs locally on the fringes of the footwall alteration zone. It has a white, flinty appearance in hand specimen and is composed of micro-crystalline quartz and K feldspar with minor sphalerite.

Mottled alteration and quartz-K-feldspar alteration facies typically show complex, gradational contacts.

Figure 3 . Geological map of the San Nicolás area. Modified after Johnson *et al.* (2000).

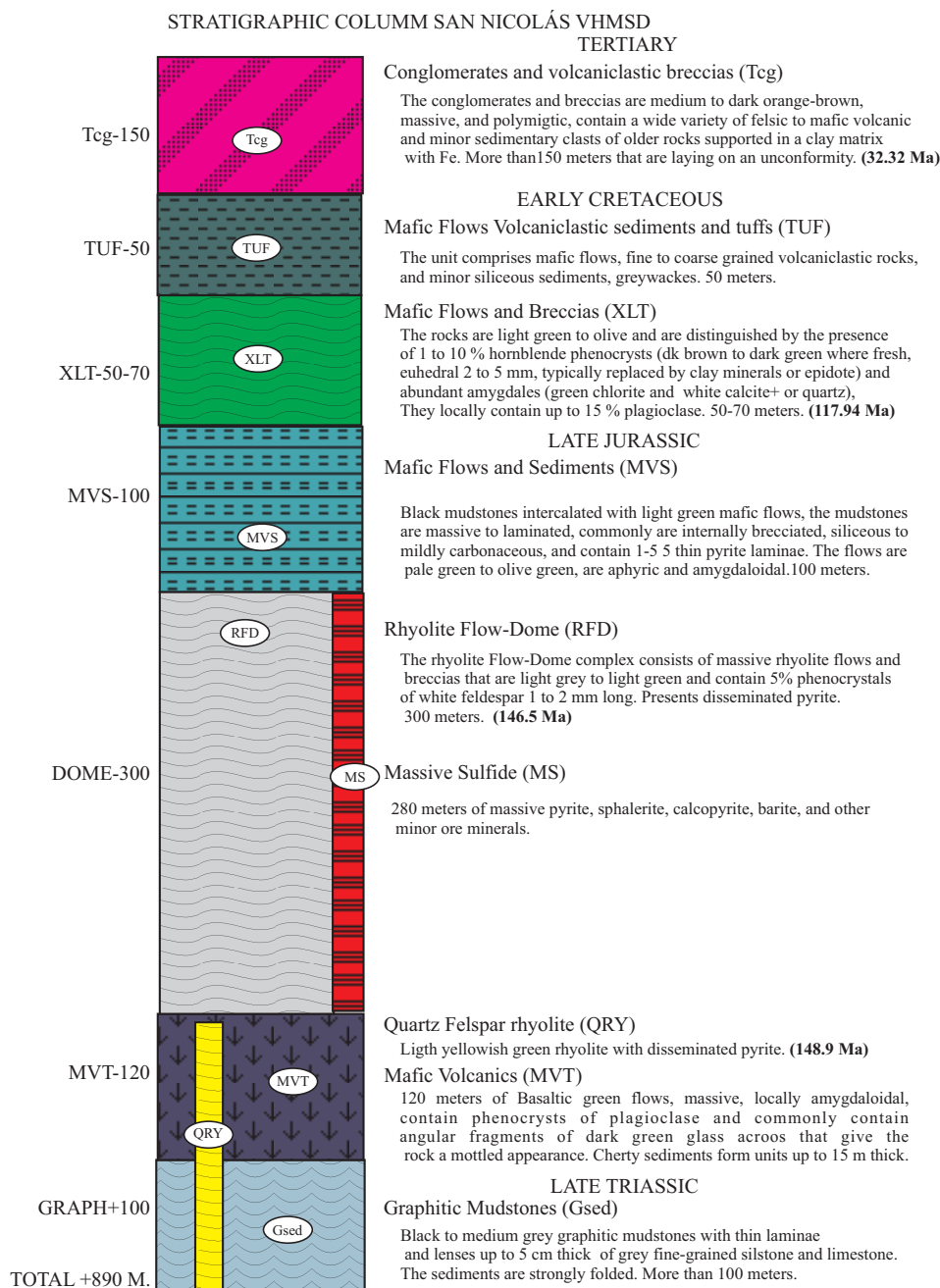
5. *Disseminated tremolite and patchy carbonate-tremolite-chlorite (Ab-calc-ep) alteration facies* (Figure 7) exist sporadically in the footwall alteration zone, generally in the top of the rhyolite lava and in association with the tectonic breccias of the San Nicolás sulfide SW lenses (Figures 6, 7). Herrmann and Hill (2001) interpreted this type of alteration facies as representing metamorphosed hydrothermal carbonate-chlorite-quartz alteration facies.

6. *Intense, quartz-pyrite (silica alteration and cpy-py stringers) alteration facies*, (Figure 7) develop stratiform bands around the massive sulfides and discordant zones within the footwall, that are interpreted as the main fluid pathways during mineralizing hydrothermal activity. Apart from relict, partly recrystallized quartz phenocrysts, the quartz-pyrite alteration facies retains no primary mineralogy or fab-

rics. This facies is dominantly siliceous with 5 to 20 % (modal) pyrite in disseminated grains and irregular veins. The total phyllosilicate content is <20 % and proportions of muscovite, chlorite and biotite are variable (Figure 8).

GEOCHEMISTRY OF ALTERATION FACIES

This section examines the major and trace element compositions of the variably altered volcanics for San Nicolás deposit. Representative analyses of least altered footwall rhyolite, quartz-eye porphyry, hanging wall dacite and the principal alteration facies are presented in Table A1 (in the electronic supplement).

Figure 4. Stratigraphic column VMS San Nicolás. Modified after Johnson *et al.* (2000).

Methods

Whole-rock chemical analyses were obtained from 100 samples of altered footwall volcanics and hanging wall rhyolites (Table A1). Crushed samples of drill core (quarter core splits, 10 cm long) were pulverized in a tungsten carbide mill. Major elements were measured by X-ray fluorescence spectrometry (XRF) on fused discs and pressed powder pellets at the ACME Laboratory in Vancouver, Canada. Concentrations of the trace elements (Ag, Bi, Cd, Sb, Cs, Tl, and U) were determined by ICP-MS, (0.5 gm sample leached with 3 ml 2-2-2 HCl-HNO₃-H₂O at 95 °C for one hour, diluted to 10 ml), REE by LiBO₂ fusion, ICP/MS finished, at the same laboratory.

Additional data were compiled from previous studies. These included analyses of carbonate-tremolite-chlorite alteration facies

from Johnson *et al.* (2000) and quartz-eye porphyry (Mortensen *et al.*, 2008). These analyses were performed at the ACME Laboratory using a combination of ICP-OES for major elements, XRF on pressed powder pellets for Zr and Ba, and atomic absorption spectroscopy (AAS) for Cu, Pb and Zn. Furthermore, supplementary analyses of altered volcanic rocks in diamond drill holes (DDH) SN-25, SN-35-37 and SN-40-41, (Table A1) were analyzed by ICP-OES for major elements, ICP-MS and INAA for trace elements, XRF on pressed powder pellets for Zr, AAS for Cu, Pb, and Zn, and Leco (infrared spectrophotometry) for S.

Major element geochemistry

The altered mafic rocks show large variations in the concentrations of Na, Ca, Mg and Fe (Figure 7, Table A1, DDH SN-25, samples

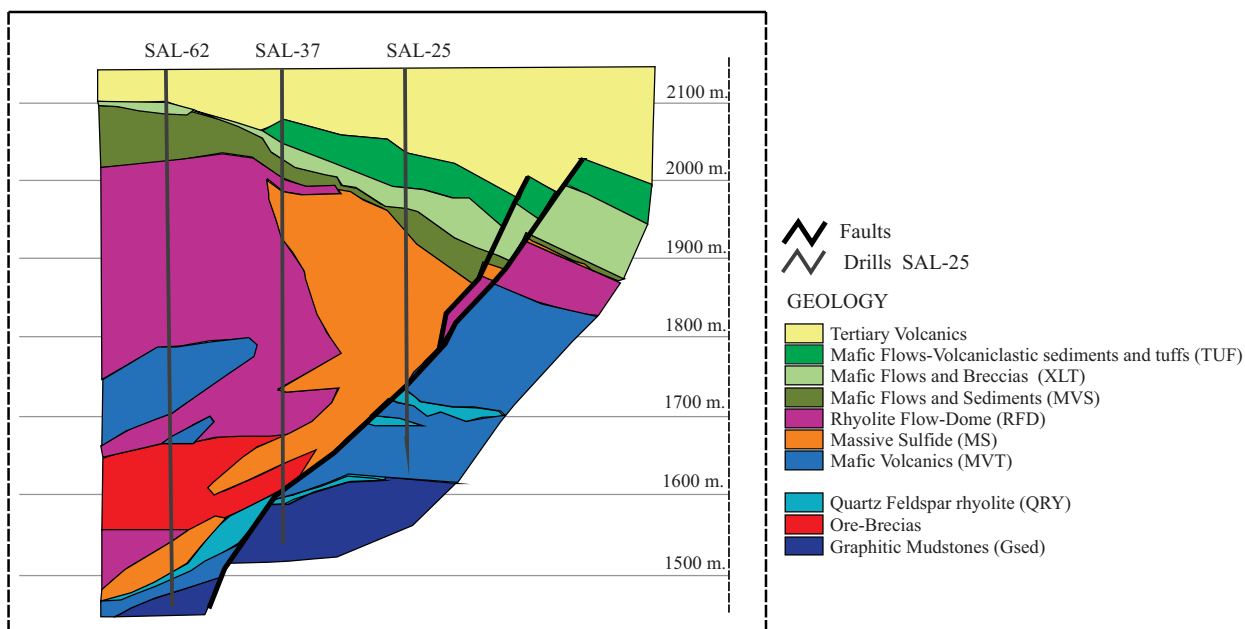


Figure 5. Cross section (SW-NE), showing the ore body and the growing fault La Panza at San Nicolás.

BSN-28-31). Least altered mafic rocks are within Mg and Fe average and contain between 3 and 8 wt % $\text{Na}_2\text{O}+\text{CaO}$, which is within the range typical for fresh modern mafic volcanics. Increasing alteration is coupled with a gradual decrease in Na_2O and CaO , culminating in intensely altered basalts having $\text{Na}_2\text{O}+\text{CaO}$ values < 1.04 wt % (sample BSN-45). This trend is indicative of plagioclase destruction and formation of muscovite (sericitization). Intense pyritic alteration facies is characterized by high $\text{MgO}+\text{FeO}$ values, commonly between 3 and 20 wt % (up to 36 wt %, sample BSN-24), due to the abundance of pyrite and chlorite. The calcareous alteration facies show extreme CaO and MgO enrichment (samples BSN-11-12, BSN-76-81, above

the ore body), which is related to a combination of carbonate (dolomite) and chlorite (Figures 9, 10). Samples of quartz-eye porphyry have $\text{MgO}+\text{Fe}_2\text{O}_3$ values mainly between 6 and 10 wt % and their $\text{Na}_2\text{O}+\text{CaO}$ content ranges between <1 and 4 wt %, (BSN-05-43) overlapping with least altered, weakly altered, and moderately altered footwall rhyolite.

The alteration facies of the San Nicolás deposit can be geochemically distinguished in one diagram, which utilizes two multielement ratios to monitor relative changes in the concentrations of MgO , FeO , K_2O , Na_2O and CaO (the alteration boxplot; Large *et al.*, 2001; Figures 9, 10). The alteration index ($\text{AI} = 100^*[\text{MgO}+\text{K}_2\text{O}]/[\text{MgO}+\text{K}_2\text{O}+\text{Na}_2\text{O}+\text{CaO}]$; Ishikawa *et al.*, 1976) quantifies Ca and Na depletion and enrich-

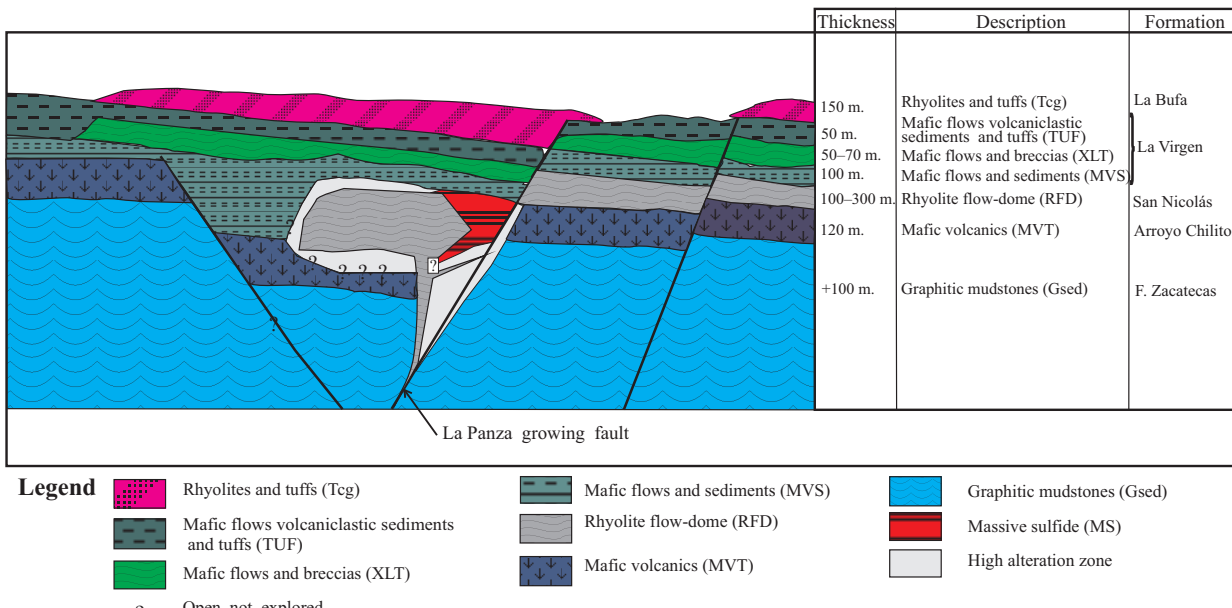


Figure 6. Model for the volcanic structure of the San Nicolás host-rock succession. Cross section SW-NE.

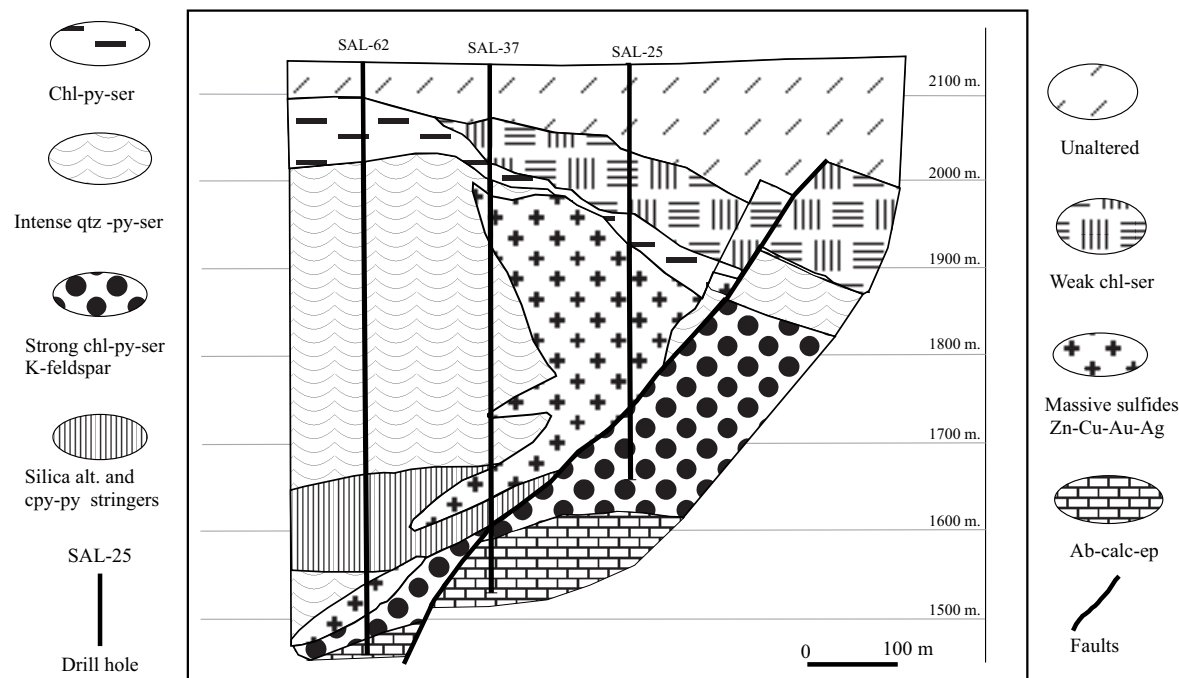


Figure 7. Alteration facies at the San Nicolás deposit. Cross section SW-NE.

ment relative to Mg and K. The AI increases as a result of plagioclase destruction or chlorite, muscovite, and K feldspar formation.

In contrast, relative K depletion due to K-feldspar alteration or Ca enrichment associated with carbonate alteration results in low AI values. On the other hand, the carbonate-chlorite-pyrite index CCPI = $100 \times [\text{MgO} + \text{FeO}] / [\text{MgO} + \text{FeO} + \text{Na}_2\text{O} + \text{K}_2\text{O}]$; measures total alkali depletion relative to Mg and Fe enrichment associated with chlorite and pyrite formation and dolomite- and/or ankerite-rich carbonate precipitation. A combination of both indices in the boxplot (Figure 10) enables discrimination of the main alteration assemblages and separates unaltered or weakly altered samples, representing background compositions, from samples with hydrothermal alteration (Large *et al.*, 2001).

Least altered footwall volcanic rocks have AI values between 28 and 36 and CCPI values between 44 and 64 (Figure 10), reflecting relatively high, primary concentrations of alkalis and low Fe and Mg concentrations (samples BSN- 26-27-28).

In contrast, intensely altered, pyrite-rich rhyolites plot in the upper right-hand corner of the boxplot (AI: >90, CCPI: 50–95). BSN-29 (CCPI=80, from 35 m to ore body), BSN-15 (CCPI=81.8 from 100 mto the ore), BSN-77 (CCPI=75.6 from 80 m to the ore), and BSN-48 (CCPI=78.8 from 83 m to ore body). The large range of CCPI is related to variations in the proportions of chlorite, biotite and muscovite.

The mottled alteration facies has intermediate AI and CCPI values, partly overlapping the fields for the least altered rhyolite and pyrite-rich alteration facies. Samples of the carbonate alteration facies plot along the upper boundary of the diagram (CCPI >90) and the large spread in AI values reflects variations in the proportions of carbonate, chlorite, and tremolite. Samples of the quartz-K feldspar alteration facies overlap with samples of the mottled alteration facies and define a trend toward the composition of K feldspar. Most samples of the hanging-wall dacite and a few samples of weakly altered footwall rhyolite have low AI values (<20), which is consistent with albite alteration. Samples of quartz-eye porphyry show a wide distribution in the alteration box-plot, with data points overlapping

with the least and weakly altered footwall rhyolites and mottled alteration facies (Figure 10).

Immobile trace element ratios—constraints on primary geochemistry

Geochemical discriminant diagrams are relatively common for mafic volcanic rocks (Pearce and Cann, 1973; Winchester and Floyd, 1977, and Wood, 1980). Discriminant diagrams are commonly (although not exclusively) based on elements that are considered to be immobile under most geologic conditions. These include selected major, trace, and rare earth elements. Some well-known discriminant diagrams use absolute concentrations of element pairs such as Zr-Y, Nb-Y, Zr-Nb, Zr-Ti, Th-Ta, Th-Yb, Th-Hf, and La-Yb, whereas others use element ratios. Because the behavior of some elements is comparable (*i.e.*, Zr and Hf, Nb and Ta, Y and Yb), these elements are commonly used on diagrams, depending on the preferred analytical technique. In order to avoid common geochemical problems associated with mass loss and mass gain caused by extensive hydrothermal alteration of the host volcanic rocks around VMS deposits, the diagrams presented are based on element ratios, rather than on element concentrations (Gorton and Schandl, 2000, Schandl and Gorton, 2002).

A Zr/TiO₂-Nb/Y discrimination diagram (Figure 11) shows that immobile element data are consistent with the classification of volcanic rocks of San Nicolás (Winchester and Floyd, 1977). Hanging wall ore-related rhyolite flow-dome (RFD) plots in the field for rhyolite despite the extensive modifications of bulk-rock composition due to alteration. This suggests that rhyolite was a typical acid rock essentially homogeneous in primary composition prior to hydrothermal alteration. The immobile element signature of hanging-wall dacite is similar to ratios of fresh volcanics of dacitic and rhyodacitic composition. Samples of quartz-eye porphyry also plot in the field for dacite and rhyodacite because of their lower Zr/TiO₂ ratios compared to footwall rhyolite. Samples of footwall strong chl-py-ser K-feldspar plot in the field for basaltic and andesite-basaltic rocks because of their lower Zr/TiO₂ ratios compared to hanging-wall weak chl-ser mafic rocks.

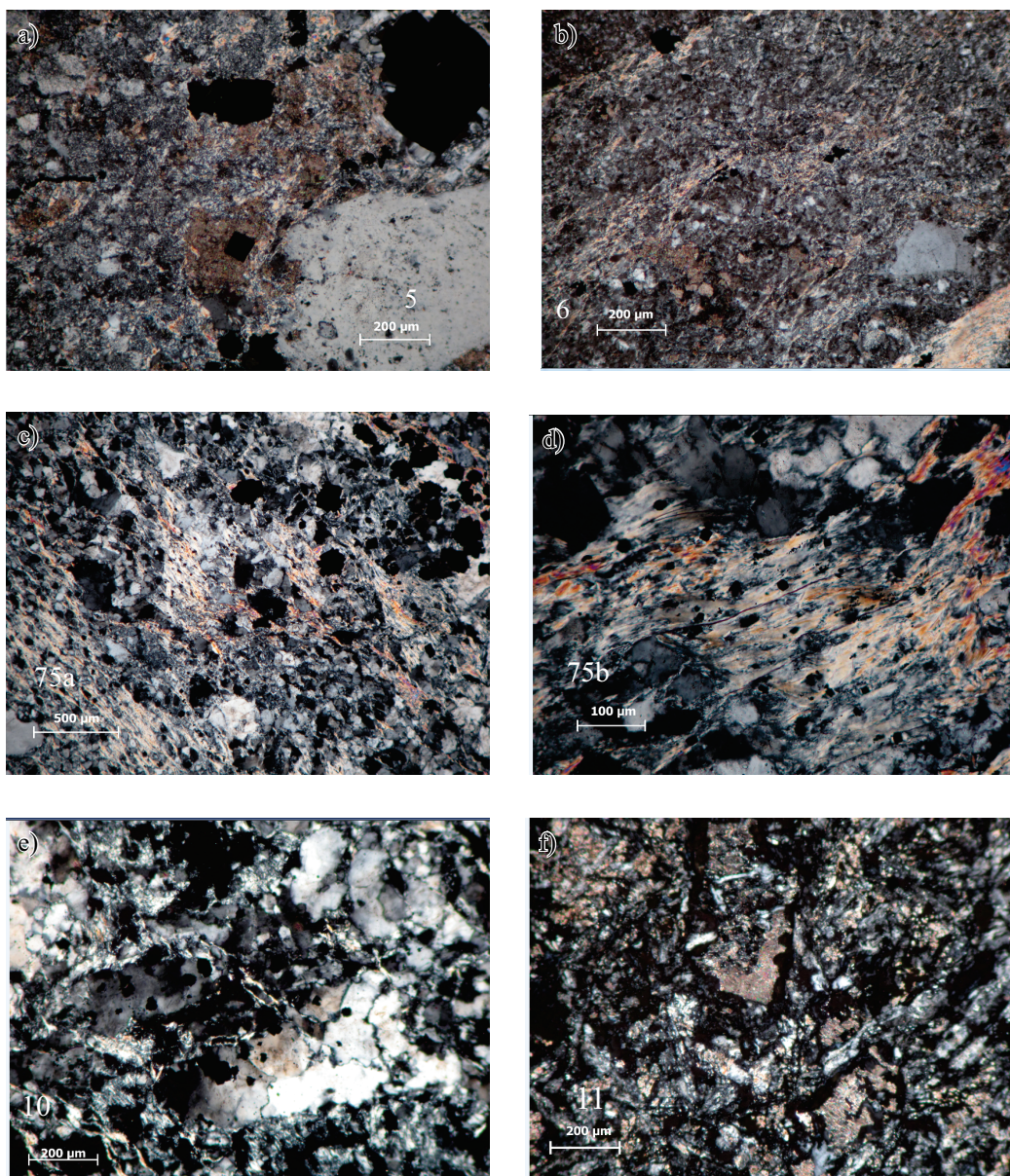


Figure 8a. Textures of volcanics at the San Nicolás deposit. Altered mafic volcanic rocks. a) BSN-05- depth 526 m (MVT), py, sericite, calcite, chlorite; b) BSN-6- depth 501 m (MVT), py, sericite, calcite, chlorite; c) BSN-75 a- depth 414 m (MVT), py, sericite, chlorite; d) BSN- 75 b- depth 414 m (MVT), py, sericite, chlorite. BSN-10- depth 412 m (MVT), py, chlorite, sericite; f) BSN-11- depth 217 m (MVS), py, sericite, qtz, chlorite. (*continues*).

Base metals and mobile trace elements

Concentrations of Cu, Pb, Zn, Ba, Rb, Sr, Tl, As, Bi, and Mo were plotted against Na₂O, because Na depletion is an indicator of increased alteration intensity in the footwall alteration zone, whereas albite-altered hanging-wall dacite has high Na₂O values (Figures 12, 13). The base metal contents of samples from the footwall alteration zone vary substantially and intensely altered rhyolite often has one order of magnitude higher Cu, Zn, and Pb concentrations than least altered rhyolite, hanging-wall dacite, and quartz-eye porphyry (Figures 12, 13). However, there is overlap and no clear correlation between alteration intensity and base metal concentrations.

Variations in Ba, Rb and Sr contents and in the Rb/Sr ratio are probably controlled by differences in mineralogical composition (Figures 12, 13). The increase in Ba and Rb from the least altered

hanging wall mafic volcanics (samples BSN-26-31) to some samples of moderately to intensely altered footwall mafic volcanics (samples BSN-41-45) may be related to the formation of muscovite and K feldspar replacing primary plagioclase with Ba and Rb for K. Thus, muscovite-poor samples of the intense quartz-pyrite-ser alteration facies (Figure 7, Table A1) have low Ba and Rb concentrations. Extremely low values for Ba and Rb occur in several Na-rich samples of the hanging wall rhyolite where albitization of feldspar led to concurrent K, Ba and Rb depletion. Samples of carbonatite alteration facies are barium-rich (commonly about 1 wt %), which is related to the occurrence of barite. The somewhat erratic variations in Sr concentrations are probably related to occurrences of epidote and calcite where Sr replaces Ca.

The concentrations of Tl, As, Bi and Mo (Figure 13, Table A2 in the electronic supplement) are close to or below the detection limit for

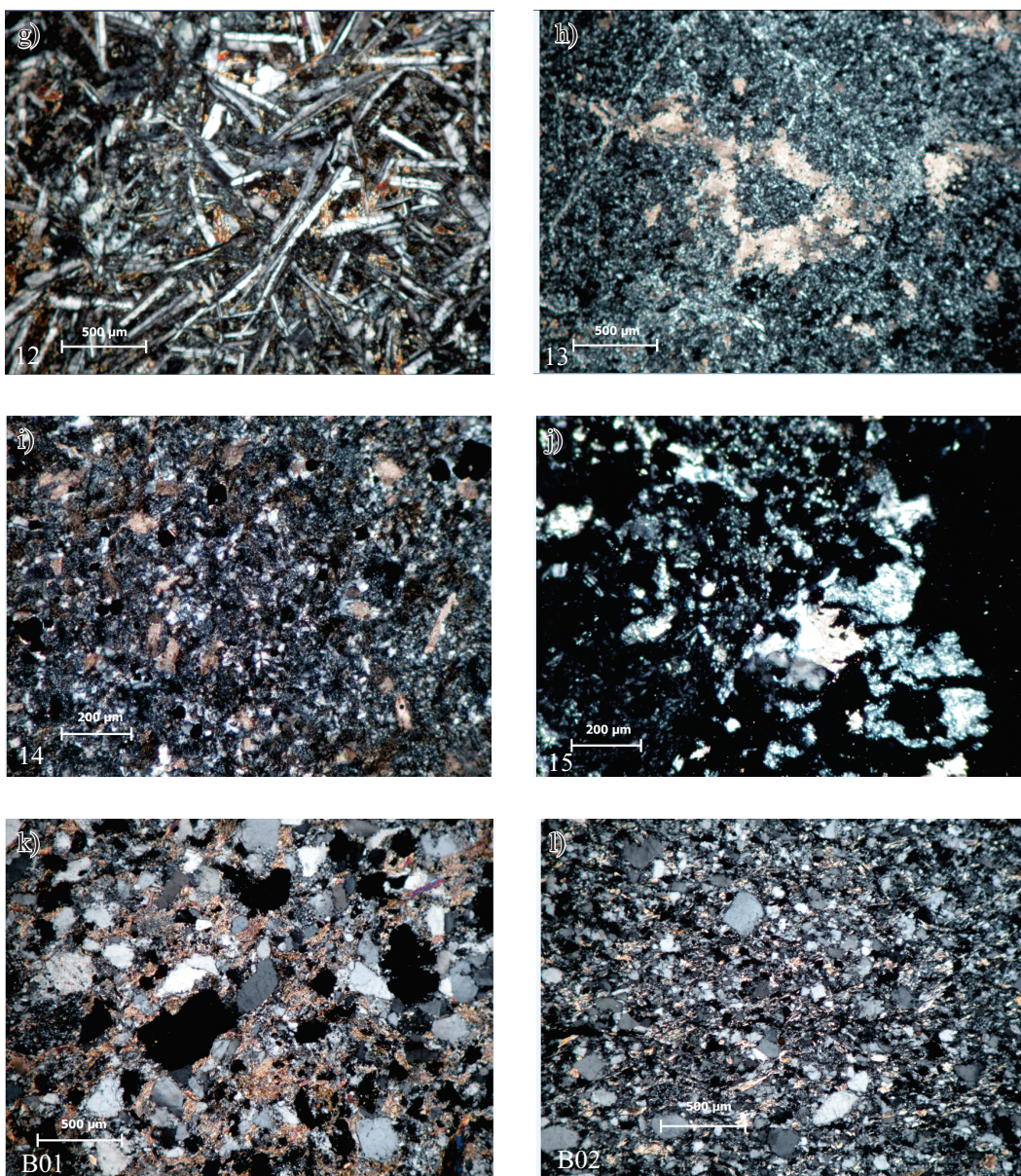


Figure 8 (cont.). Textures of volcanics at the San Nicolás deposit; g) BSN-12- depth 188 m (MVS), plagioclase, sericite, chlorite; h) BSN-13- depth 164 m (MVS), py, sericite, calcite, chlorite; i) BSN-14 - depth 145 m Mafic flows (XLT), py, calcite, sericite, chlorite; j) BSN-15- depth 125 m Mafic flows, volcaniclastic sediments and tuffs (TUF), Basalt with low alteration, qtz, calcite, k) B01- superficial sample, greywackes (TUF) with: py, chlorite, sericite; l) B02 - superficial sample, sandstone (TUF) with: py, sericite, qtz, chlorite.

most samples with Na_2O values higher than approximately 1 wt %. In contrast, samples of altered rhyolite, with $\text{Na}_2\text{O} < 2$ wt % show a large range of variation of As with maximum values typically 10 to 15 times higher than in least altered rhyolite.

GEOCHEMICAL INDICATORS OF PROXIMITY TO THE SAN NICOLÁS DEPOSIT

Representative drill holes from San Nicolás deposit were selected to illustrate the relationship between geochemical changes and proximity to the massive sulfide lenses. The orientation of these drill holes with regard to the San Nicolás Formation (rhyolite flow-dome, RFD in Figure 4) is variable. (Figure 7). Drill hole SAL-25 was collared in no

altered hanging wall rhyolite ~220 m over the San Nicolás Formation. Drill hole SAL-35 (100 m to the south-west of the section in figures 3, 5) cuts 245 m of several zones of quartz-pyrite alteration facies. This drill hole starts in no altered basalts and ends with quartz-K feldspar alteration facies ~40 m stratigraphically below the San Nicolás Formation. Drill hole SAL-25 was selected to examine the geochemistry of a thick lava unit directly overlying the massive sulfides in San Nicolás deposit.

Footwall halo

Major elements and alteration indexes

The data from drill hole SAL-25 illustrate the geochemical variability of the San Nicolás alteration zone in the hanging wall (samples BSN-41-45), which is characterized by elevated values for MgO , S ,

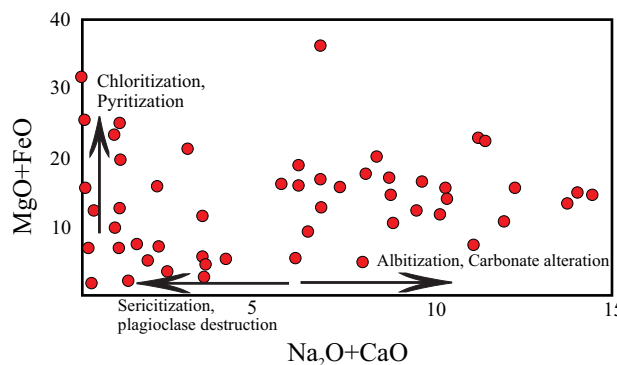


Figure 9. The alteration and variations in the concentrations of Na, Ca, Mg, and Fe. The composition of moderately to intensely altered footwall rhyolite indicates that hydrothermal alteration was dominated by processes such as destruction of primary feldspar, sericitization, chloritization, and pyritization leading to Na₂O loss and elevated values for MgO+FeO.

AI, and CCPI in San Nicolás due to the abundance of chlorite-rich quartz-pyrite alteration facies.

In drill hole SAL-25, the vertical concentration of Na₂O decreases toward the San Nicolás Formation and values <1 wt % are common in the upper part of the mottled alteration facies between 384 to 420 m (Table A1, Figure 14). The concentration of MgO increases from regional background levels (2-3 wt %) to values around 9.82 wt % in the central part of the alteration zone. Alteration index and CCPI values are close to values typical (35-64) for the least altered rhyolite in the lower part of the mottled alteration facies but increase toward the San Nicolás Formation sulfides (203 m depth) (45-80). Sulfur concentrations are high (2.61 %) at the quartz-pyrite alteration facies just below the massive ore body (384 m), and low (0.03 wt %) over the sulfides (203 m).

In drill hole SAL-25, Na₂O values are below 1.62 wt % for most samples and AI values >61.4 predominate (Figures 6, 14). A drop in AI

values just below the San Nicolás Formation (203 m depth) is correlated with a tremolite and barite-rich sample of strong chl-py-ser-K-feldspar alteration facies. The pattern for S drops from 2.61 wt % to almost zero, although most samples have concentrations <1 wt % and one zone of chl-py-ser-K-feldspar alteration facies has exceptionally high S values (≥ 2 wt %). This zone is also marked by peaks in MgO concentrations (3.0 and 9.82 wt %). In contrast, the CCPI values increase smoothly from 43 at the start of drill core SAL-25 to values >79 just below the ore.

Increase of MgO, AI and CCPI and depletion of Na₂O and S are characteristic geochemical features for the San Nicolás footwall alteration zone. The potential of these parameters to be a guide in base metal exploration is variable and depends on the specific alteration facies present. In San Nicolás, the smooth increase in CCPI (BSN-29-31) is an excellent guide to ore, due to intense Na₂O depletion and abundance of chlorite-rich quartz-pyrite alteration facies. Also, a comparatively smooth trend in Na₂O depletion and a relatively subtle increase in CCPI (from 25-50) are observed when approaching massive sulfides orebodies in any direction, up or down (Table A1).

Base metals

Concentrations of base metals in altered rhyolite show erratic variations with comparable ranges in San Nicolás. Although values higher than background are predominant, numerous samples show base metal concentrations within the range of the least altered rhyolite. There are no consistent trends in the base metal data that could be used as a guide to the massive sulfides in San Nicolás. Consequently, analyses of Cu, Pb, and Zn have a low potential as vectors to ore (Figure 14).

Trace elements

In general, concentrations of Ba show consistent changes with distance from the San Nicolás favorable unit, and increases with CCPI values. Ba-rich samples in the vicinity of massive sulfides are potentially useful as mine-scale exploration vectors and correlate with local occurrences of barite. In San Nicolás the chlorite-rich quartz-pyrite alteration facies are marked by strong depletion in Ba. A general increase in the Rb/Sr ratio can be observed in all the ore body of San

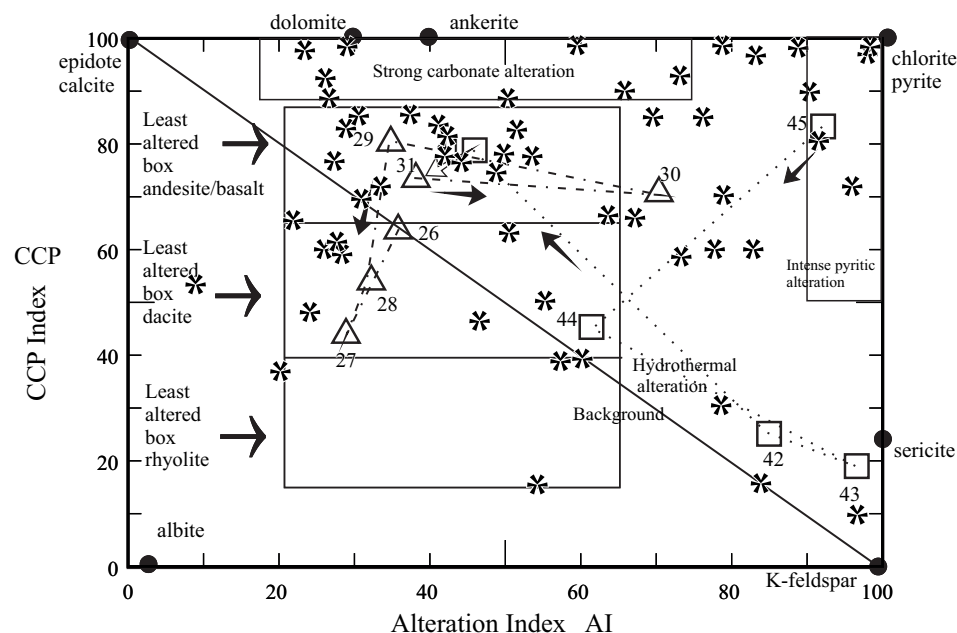


Figure 10. The alteration facies at San Nicolás, DDH (diamond drill hole) SAL-25 (samples 45-41 under ore; 31-26 above ore, arrows are from bottom to surface), with alteration facies box-plot (Large *et al.*, 2001). Stars represent other drill samples. (see Table A1 in the electronic supplement).

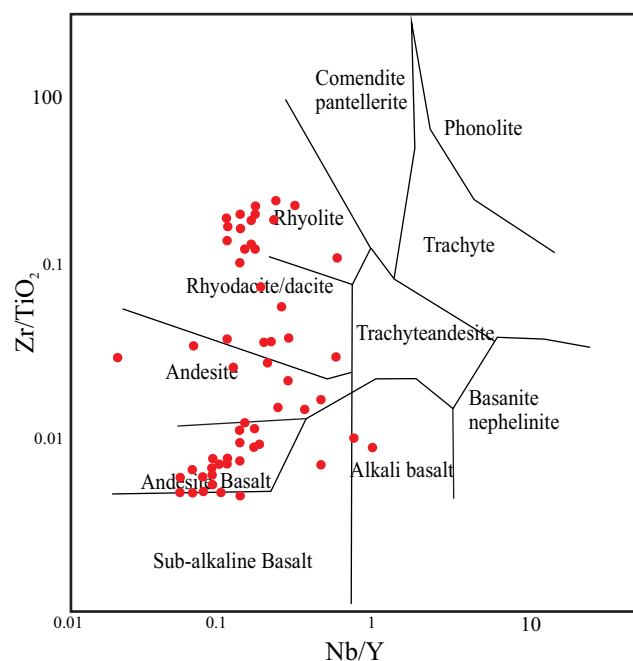


Figure 11. Immobile element data are consistent with the field classification of volcanics at San Nicolás and are not influenced by alteration.

Nicolás; however, there is considerable scattering and overlapping with the range for the least altered rhyolite. Just below the San Nicolás favorable unit, the Rb/Sr ratio decreases dramatically to the presence of disseminated tremolite alteration facies. The concentrations of Mo, Bi, and As are typically less than 1 ppm in the least altered footwall rhyolite. In contrast, altered footwall rhyolites often contain several to >10 ppm of these elements. In San Nicolás, the concentrations of these elements vary erratically and a correlation with distance from ore is not apparent. In the west part of San Nicolás, elevated values of Mo and As (>10 ppm) are restricted to the quartz-pyrite alteration facies immediately below massive sulfides. In general, Tl concentrations are close to, or below, the detection limit (<0.5 ppm) for all samples regardless of alteration facies. However, elevated Tl values (>3 ppm) occur in samples just at the beginning of the San Nicolás favorable unit in drill hole SAL-25 (from 210 to 380 m, Figure 14).

Ba concentrations are strongly controlled by mineralogy of alteration (*i.e.*, abundance of muscovite, K feldspar, or barite) and may be enriched or depleted in the hanging wall alteration zone compared to the least altered footwall volcanic rocks. It is typical that Ba is concentrated in the upper parts of ore bodies, but its concentration is depleted at the lower parts where Cu is abundant. The Sr is a good indicator of feldspar-destructive alteration and generally increases toward the San Nicolás favorable unit. However, the occurrence of Ca-bearing minerals (epidote, calcite, tremolite) have a strong effect, causing substantial distortion of the trend in drill holes SAL-25 (samples BSN-41-51), and SAL-35 (samples BSN-3-24-25). Elevated concentrations of Mo, Bi and As distinguish the footwall alteration zone from the surrounding least altered rhyolite and may be useful in district-scale base metal exploration (Figures 12, 13).

Hanging wall halo

The hanging wall andesite lavas in drill hole SAL-37 are relatively homogeneous in geochemical composition (Table A1). However, high Na₂O values (2.6–3.3 wt %) and alteration index AI=36 indicate

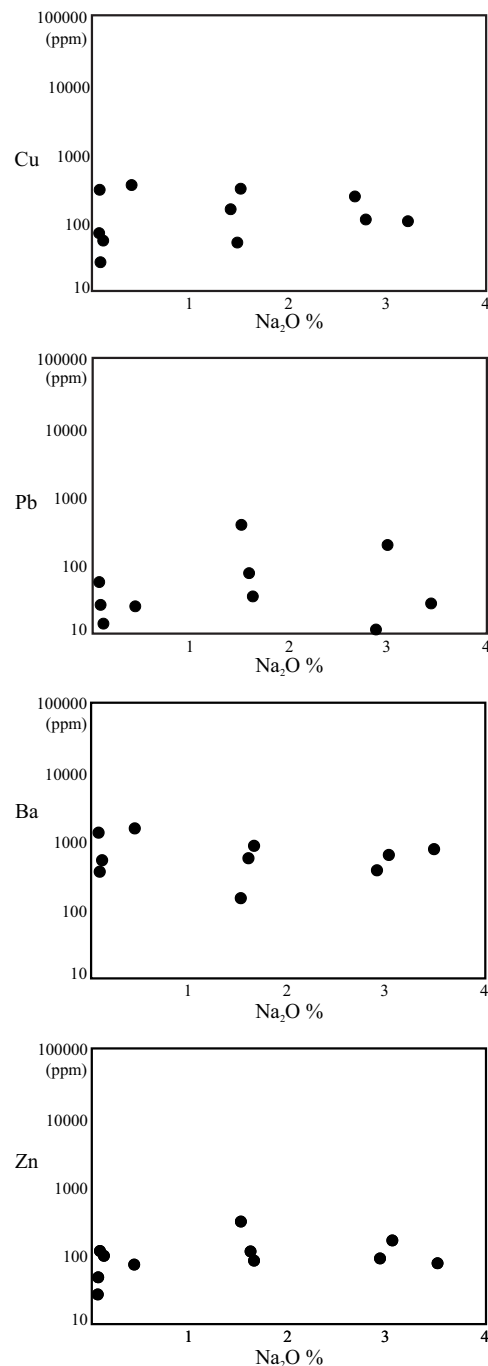


Figure 12. Concentrations of Cu, Pb, Zn, and Ce for SAL-25 DDH, in hanging-wall rhyolite, and quartz-eye porphyry. The decreasing concentration of Na₂O is an indicator of increased intensity of hydrothermal alteration.

albite alteration in its upper part, which is also accompanied by low concentrations of Ba. Increasing albite alteration in samples near to the San Nicolás favorable unit indicates that this type of alteration is related to the hydrothermal activity associated with mineralization at San Nicolás. Nevertheless, andesite sampled at approximately 50 m stratigraphically above the San Nicolás favorable unit (SAL-25, 240 m; Figure 14) shows elevated concentrations of Zn, Pb, and Bi compared to mafic flows higher in the sequence. This sample also contains sulfur (0.07 wt %), which is unusual because, in general, rhyolite is

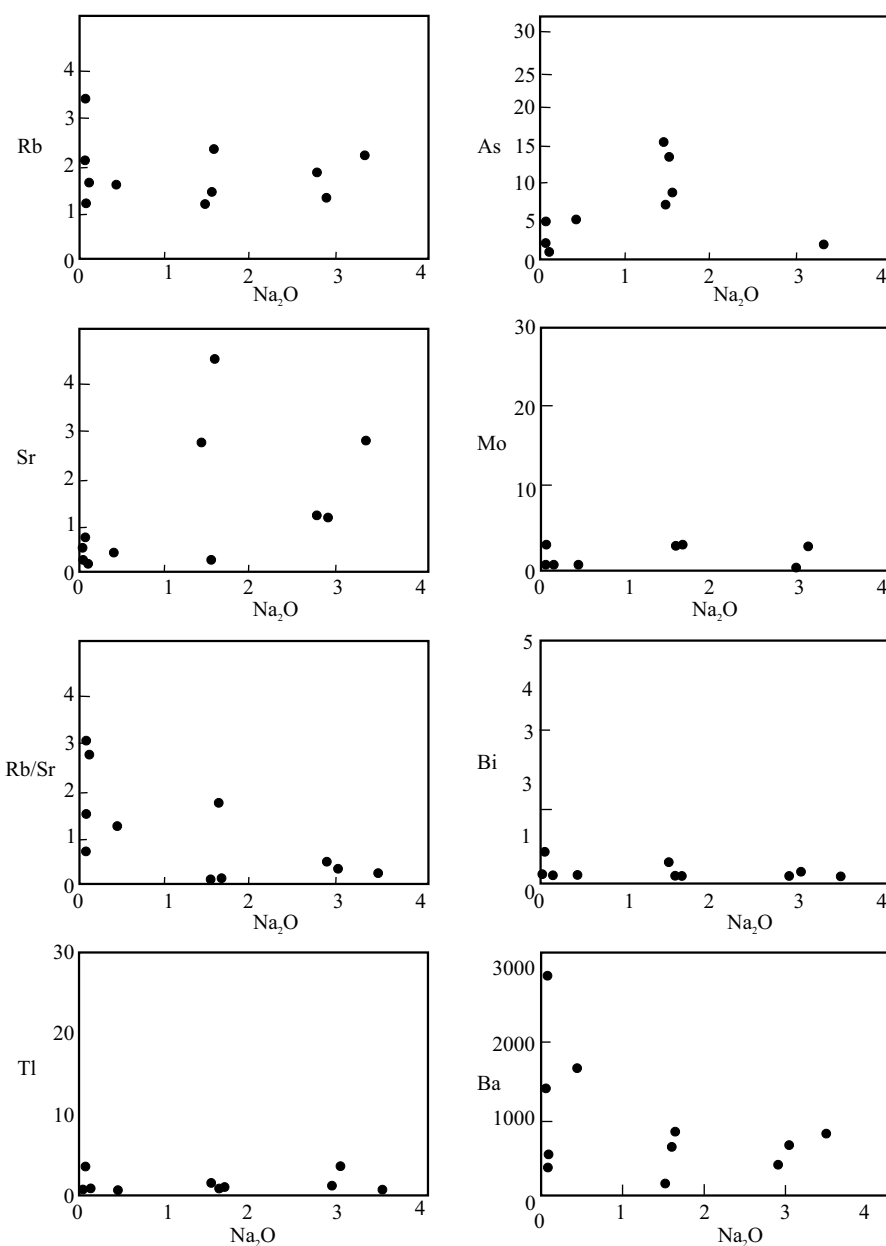


Figure 13. Variation diagrams for SAL-25 DDH showing the variability of trace element concentrations in hanging-wall rhyolite and quartz-eye porphyry (Rb, Sr, Rb/Sr, Tl, As, Mo, Bi and Ba ppm vs. $\text{Na}_2\text{O}\text{ %}$).

extremely sulfur-poor with values generally below the detection limit (<0.01 wt %). This enrichment in S, Zn, Pb and Bi may be related to localized late activity of the San Nicolás hydrothermal system.

DISCUSSION

Hydrothermal alteration of the volcanic rocks

The San Nicolás alteration zone consists of six alteration facies with a distinctive mineralogical and geochemical characteristics. Based on geological, mineralogical and geochemical data, a conceptual model for the evolution of the San Nicolás hydrothermal system is presented (Figure 7). Although a temporal evolution of the hydrothermal system is suggested, other alteration processes may have occurred concurrently in different parts of the system.

Carbonate alteration

The origin of the carbonate alteration has been examined in detail by Herrmann and Hill (2001) at the Thalanga deposit, Australia, who concluded that carbonate-tremolite-chlorite alteration facies represents the metamorphic equivalent of intense chlorite-calcite \pm dolomite alteration, which occurred in footwall rocks close to the sea floor by a process involving mixing of hydrothermal fluids and seawater.

The abundance of the carbonate-tremolite-chlorite alteration facies in central San Nicolás suggests that the volcaniclastic units and the fault pathway (Figures 5, 10) provided favorable conditions for mixing of upwelling hydrothermal fluids with ambient seawater.

Hydrothermal carbonate alteration is common in VMS deposits and has been described from several deposits in Tasmania, such as Rosebery deposit, (Lees *et al.*, 1990); Hercules deposit, (Zaw and Large, 1992); Hellyer deposit, (Gemmell and Large, 1992), in VMS

russian districts (Smirnov, 1968, 1976; Smirnov and Gorzhevskii, 1978; Starostin, 1984), in Chisel Lake, Canada, (Galley *et al.*, 1993), and in Kuroko, Japan (Shikazono *et al.*, 1998). It has also been observed in modern, submarine hydrothermal systems Middle Valley, northern Juan de Fuca Ridge, (Goodfellow *et al.*, 1993). In general, oxidizing conditions and low temperatures (<200 °C) are inferred for carbonate alteration. By analogy, carbonate alteration at San Nicolás is interpreted to represent a relatively low temperature process, which occurred at an early stage during the development of the San Nicolás hydrothermal system (Figures 7, and 10).

Phyllosilicate-dominated alteration

Feldspar-destructive, muscovite-chlorite-biotite-rich mottled (strong chl-py-ser K-feldspar) alteration facies, (Figure 7). The bulk of the footwall alteration zone consists of the mottled facies, which shows destruction of primary feldspars, formation of hydrothermal phyllosilicates, and precipitation of disseminated pyrite. In comparison mineral assemblages in modern submarine hydrothermal systems with sulfide mineralization on the seafloor suggests that hydrothermal phyllosilicates included sericite, chlorite and clay minerals, such as illite and smectite (Binns and Scott, 1993). The muscovite-chlorite-biotite mineral assemblages observed in mottled alteration facies represent the metamorphic equivalents of these hydrothermal phyllosilicates.

The textural diversity of the mottled alteration facies and the abundance of apparent clastic textures indicate that multistage alteration processes were common. These processes may have been related to variations in fluid composition, temperature and changing water/rock ratios. The continuous lateral extent of the mottled alteration facies suggests that upwelling of hydrothermal fluids was diffuse (Figure 8).

The mottled alteration facies has been intersected by drill holes down to a stratigraphic depth of at least 150 m below the San Nicolás favorable unit (Figure 10); however, its full extent into the footwall is unknown. Broad, feldspar-destructive alteration zones of similar lateral dimensions as at San Nicolás have been recognized below Mesozoic VMS deposits in the Francisco I. Madero district, in central Zacatecas, (Vassallo, 1995). These can be traced for up to 300 m into the footwall stratigraphy where they become narrower and more confined. Hence, the apparently stratabound footwall alteration zone at San Nicolás may represent the upper part of a similarly broad, transgressive zone of hydrothermal fluid upflow.

Quartz-K feldspar alteration facies type has rarely been reported from alteration zones associated with VMS deposits. Nevertheless, K feldspar has been observed in the outer parts of alteration systems associated with the Kuroko deposits in Japan (Shirozo, 1974, Shikazono *et al.* 2008) and the Que River deposit, Tasmania, Australia, (McGoldrick and Large, 1992). At Que River, K feldspar is associated with silicification and Au-rich mineralization, interpreted to have formed by mixing of ore fluids of moderate temperature (200–250 °C) and seawater.

By analogy with these studies and based on the observation that quartz-K feldspar alteration facies is restricted to the outer (cooler?) parts of the San Nicolás hydrothermal system, it is inferred that this type of alteration took place under relatively low temperature conditions and low water/rock ratios. The formation of K feldspar rather than sericite suggests that the pH of the hydrothermal fluids increased from acidic in the central parts of the hydrothermal alteration system to near-neutral on its fringes.

It is inferred that mixing of hydrothermal fluids with seawater at the margin of the hydrothermal system could have caused simultaneous cooling and neutralization of the fluid, resulting in the formation of the quartz-K feldspar alteration facies. Variations in the influx rate, temperature, composition, and pathways of the hydrothermal fluids

probably led to changes in the location of quartz-K feldspar alteration and, overprinting with the mottled alteration facies.

Mineralizing alteration

The fault zone of the quartz-pyrite alteration facies is interpreted to represent the principal pathways of hydrothermal fluids during mineralizing hydrothermal activity (Figures 5, 6). This interpretation is supported by the high abundance of disseminated pyrite and pyrite veins, the substantially elevated concentrations of S, base metals, and trace elements, such as As, Mo, and Bi, and the observed connection between massive sulfides and quartz-pyrite alteration facies. However, the mechanism that controlled discharge of hydrothermal fluids at San Nicolás is the growing faults systems. Synvolcanic faults have been recognized (Vassallo, 2003), and a comparison of volcanic facies architecture and the distribution of alteration facies showed that intense hydrothermal fluid flow was controlled by Jurassic faulting and in part by lithofacies. The mineralizing event was between 148.9 Ma and 146.5 Ma, whereas all the volcanic process involved lasted from 148.9 Ma to 117.94 Ma, about 31 Ma (Figure 4).

The quartz-pyrite alteration facies also exists as stratiform zones immediately below the massive sulfides. These probably formed as a result of lateral flow of hydrothermal fluids below the paleo-seafloor. This process appears to have been particularly important in southern part of San Nicolás where the stratiform ore zone is up to 50 m thick (Figures 5, 6).

In contrast to the quartz-pyrite alteration facies, which is ubiquitous below the lowest San Nicolás sulfide lenses, the chlorite-pyrite alteration facies is restricted to a narrow zone underlying massive sulfides in San Nicolás (Figures 5, 6). This alteration facies (samples BSN-07-08) is distinctive in having the highest enrichment in Mg, Fe, and substantial depletion of SiO₂. Possibly, a relatively short lived episode of hydrothermal alteration characterized by Mg-rich, Si-poor fluids forming zones of chlorite-pyrite alteration facies occurred in upper San Nicolás. Subsequently, the conditions of alteration and/or the composition of the hydrothermal fluid may have changed promoting quartz-pyrite alteration.

Geochemical proximity indicators to the San Nicolás deposit

The footwall geochemical halo of the San Nicolás deposit can be divided into an outer and an inner zone (Figures 5, 6). Furthermore, a small hanging wall halo was locally developed. Notwithstanding the mineralogical and geochemical variability of altered rhyolite there are several geochemical features that distinguish hydrothermally altered rhyolite from the surrounding, least altered volcanic rocks and are therefore important for the recognition of ancient, mineralizing hydrothermal systems in felsic volcanic successions. These include elevated MgO, S, Al, CCPI, Rb/Sr, Mo, Bi and As, and depletion of Na₂O.

Some geochemical parameters show well-constrained correlations with proximity to ore at San Nicolás. For example, the CCPI values increase steadily from background values from 25 to values >90 just below the San Nicolás favorable unit in San Nicolás. High values of Ti, Ba, S, Al, CCPI, Rb/Sr, Mo, or As indicate immediate proximity to ore defining the inner footwall halo (Table A1, A2).

Alteration of the hanging-wall volcaniclastic rocks is generally characterized by weak alteration facies, which formed as a result of background alteration processes unrelated to the mineralizing hydrothermal system. Nevertheless, rare minor geochemical anomalies (elevated S, Zn, Pb, and Bi) in basalt 50 m above the massive sulfides suggest that some late-stage hydrothermal activity was locally ongoing at the time of basalts emplacement in lower Cretaceous, or when the faults were still moving during Cretaceous time (Figure 14).

SAL-25

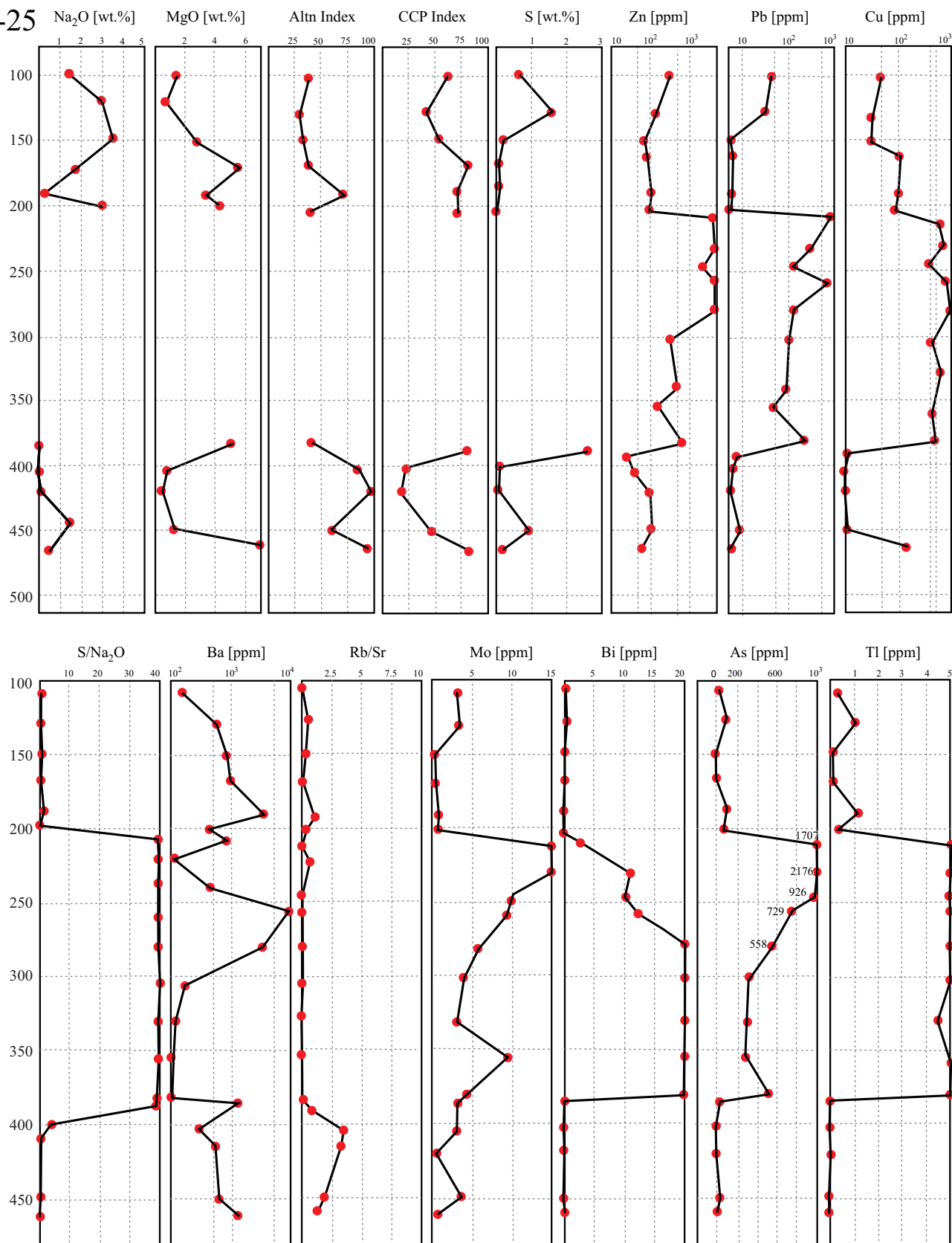


Figure 14. Geologic logs and geochemical data for SAL-25 DDH through the hanging wall and footwall alteration zone in San Nicolás. The orebody is between 204 and 383 m deep, a vertical distance of 179 m.

CONCLUSIONS

A stratabound footwall alteration zone underlies the San Nicolás massive sulfide lenses and extends for at least 200 m stratigraphically below the deposit. It envelops discordant zones of intense hydrothermal alteration, which are directly connected to the massive sulfides ore lenses in the San Nicolás rhyolite Formation (146.5 Ma). Textural, mineralogical and geochemical evidence indicates that hydrothermal alteration in the footwall involved destruction of primary feldspar, silicification and formation of pyrite, calcite \pm dolomite, K feldspar, and phyllosilicate (chlorite, sericite and clay minerals).

There are 6 alteration facies (Figure 7) from weak to intense degree: 1. Weak chlorite-sericite (weak chl-ser) alteration. 2. Chlorite-pyrite-sericite (chl-py-ser) alteration. 3. Feldspar-destructive, muscovite-chlorite-biotite-rich mottled (strong chl-py-ser K-feldspar) alteration facies. 4. The quartz-K feldspar (intense qtz-py-ser) alteration facies. 5. Disseminated tremolite and patchy carbonate-tremolite-chlorite (Ab-calc-ep) alteration facies. 6. Intense, quartz-pyrite (silica alteration and cpy-py stringers) alteration facies.

These alteration facies diversity implies that the development of the San Nicolás hydrothermal system was a complex process, probably influenced by volcanic facies architecture, fluctuations in the supply of hydrothermal fluids, changes in fluid temperature and composition, variable water/rock ratios, and interaction of hydrothermal fluids with seawater.

Chlorite-carbonate alteration facies of variable intensity was the premetamorphic precursor to the disseminated tremolite alteration facies and carbonate-tremolite-chlorite alteration facies, which formed in the near seafloor environment. Diffuse upwelling of acidic, seawater-derived hydrothermal fluids caused destruction of primary feldspar, precipitation of pyrite and formation of hydrothermal phyllosilicates (muscovite-chlorite-biotite facies) in a broad zone below the paleo-seafloor, presently occupied by the mottled alteration facies. Intense hydrothermal alteration, represented by quartz-pyrite alteration facies, exists in both discordant zones crosscutting the footwall and in stratiform zones immediately below the massive sulfide lenses. This alteration facies is inferred to have formed during mineralizing hydrothermal activity, and the fault zones are interpreted as feeder zones supplying metal-rich fluids to several hydrothermal fields separated in space along several Jurassic faults (Figures 6, and 7).

The geochemical composition of the altered rhyolite in the San Nicolás footwall alteration zone is strongly variable, reflecting the diversity of alteration processes during hydrothermal activity. However, regardless of alteration facies, Na₂O depletion is an ubiquitous feature of moderate to strong hydrothermal alteration at San Nicolás. This is commonly coupled with an increase in Al values (except for carbonate alteration as seen in Figure 10). Moderately altered rhyolite represents the bulk of the footwall alteration zone, and is geochemically characterized by elevated values for Mg, Rb/Sr, Al, CCPI and trace elements, such as Mo, Bi and As. Immediate proximity to the massive sulfides is typically indicated by elevated As, Mo, and Tl concentrations and Ba enrichment. These geochemical characteristics, together with geologic and petrographic observations, may provide useful tools for the recognition of ancient mineralizing hydrothermal systems in felsic volcanic sequences and may help to guide exploration for massive-sulfide deposits at the central part of Mexico along the Jurassic faults.

ACKNOWLEDGMENTS

Many thanks are due to the staff of Minera Teck S.A. de C.V. Guadalajara-Zacatecas; Lomonosov-Moscow State University,

Moscow, Russian Federation, provided funding for a sabbatical at Dept. of Geology, Geochemistry and Economics of Mineral Deposits, Geological Faculty, Professor Viktor I. Starostin is gratefully acknowledged. Perceptive and constructive suggestions by two anonymous reviewers considerably improved the manuscript. As always, the writers are indebted to the mineral industry for allowing access to its mineral properties and permitting extensive discussions with its geological staff. Teresa Soledad Medina-Malagón, Nancy Retiz-Vázquez, Sara Solís-Valdés, and Juan Tomás Vázquez-Ramírez of UNAM helped in many ways.

APPENDIX. SUPPLEMENTARY DATA

Tables A1 and A2 (chemical analysis of altered rocks from San Nicolás) can be found at the journal web site <<http://rmcg.unam.mx/>>, in the table of contents of this issue.

REFERENCES

Anderson, T.H., Silver, L. T., 1979, The role of the Mojave-Sonora Megashare in the tectonic evolution of northern Mexico, in Anderson, T.H., Roldán-Quintana, J. (eds.) Geology of northern Sonora: Hermosillo, Universidad Nacional Autónoma de México, Instituto de Geología, 59-68.

Allen, R.L., 1988, False pyroclastic textures in altered silicic lavas, with implications for volcanic-associated mineralization: Economic Geology, 83, 1424-1446.

Aranda-Gómez, J.J., Molina-Garza, R., McDowell, F.W., Vassallo, L.F., Ortega-Rivera, M.A., Solorio-Munguía, J.G., Aguilón-Robles, A., 2007, The relationships between volcanism and extension in the Mesa Central: the case of Pinos, Zacatecas, Mexico: Revista Mexicana de Ciencias Geológicas, 24(2), 216-233.

Aranda-Gómez, J.J., Dávila-Harris, P., Vassallo-Morales, L.F., Godchaux, M., Bonnichsen, B., Martínez-Reyes, J., Aguirre-Díaz, G., 2012, Geology and tectonics of the southeastern portion of the Sierra de Guanajuato: Field trip Guidebook 108th Annual Meeting of the Cordilleran Section of the Geological Society of America. GSA, 108th Annual Meeting of the GSA, Estados Unidos de América.

Barrett, T.J., MacLean, W.H., 1994, Mass changes in hydrothermal alteration zones associated with VMS deposits of the Noranda area: Exploration and Mining Geology, 3, 131-160.

Binns, R.A., Scott, S.D., 1993, Actively forming polymetallic sulfide deposits associated with felsic volcanic rocks in the eastern Manus back-arc basin, Papua New Guinea: Economic Geology, 88, 2226-2232.

Chávez-Cabello, G., 2005, Deformación y Magmatismo Cenozoicos en el Sur de la Cuenca de Sabinas, Coahuila, México: Universidad Nacional Autónoma de Mexico, Doctor en Ciencias de la Tierra thesis, 313 pp.

Danielson, T., 2000, Age, paleotectonic setting and common Pb isotope signature of the San Nicolás volcanogenic massive sulfide deposit, southeastern Zacatcas State, central Mexico: Vancouver, British Columbia, Canada, University of British Columbia, M.Sc. thesis, 120 pp.

De Cserna, Z., 1976a, Mexico geotectonics and mineral deposits: New Mexico Geological Society, Special Publication, 6, 18-25.

De Cserna, Z., 1976b, Geology of the Fresnillo area, Zacatecas, Mexico: Geological Society of America Bulletin, 87, 1191-1199.

Dergachev, A.L., Eremin, N.I., 2008, Volcanogenic Massive Sulfide and Exhalation-Sedimentary Lead-Zinc Ore Formation during the Earth's History: Doklady Earth Sciences, (423), No. 8, pp. 1220-1222, Original Russian Text A.L. Dergachev, N.I. Eremin, 2008, published in Doklady Akademii Nauk 2008, 423, 1, 89-91.

Eastoe, C.J., Solomon, M., Walshe, J.L., 1987, District-scale alteration associated with massive sulfide deposits in the Mount Read Volcanics, western Tasmania: Economic Geology, 82, 1239-1258.

Franklin, J.M., Lydon, J.W., Sangster, D.F., 1981, Volcanic-associated massive sulfide deposits: Economic Geology, 75th Anniversary Volume, 485-627.

Freydier, C., Lapierre, H., Briquet, L., Tardy, M., Coulon, C., Martinez-Reyes, J., 1997, Volcaniclastic sequences with continental affinities within the Late

Jurassic-Early Cretaceous Guerrero intra-oceanic arc terrane (Western Mexico): *Journal of Geology*, 105, 483-502.

Freydier, C., Lapierre, H., Ruiz, J., Tardy, M., Martinez-R. J., Coulon, C., 2000, The Early Cretaceous Arperos basin: an oceanic domain dividing the Guerrero arc from nuclear Mexico evidenced by the geochemistry of the lavas and sediments: *Journal of South American Earth Sciences*, 13, 325-336.

Galley, A.G., Bailes, A.H., Kitzler, G., 1993, Geological setting and hydrothermal evolution of the Chisel Lake and North Chisel Zn-Pb-Cu-Ag-Au massive sulfide deposits, Snow Lake, Manitoba: *Exploration and Mining Geology*, 2, 271-295.

Gemmell, J.B., Large, R.R., 1992, Stringer system and alteration zones underlying the Hellyer volcanogenic massive sulfide deposit, Tasmania, Australia: *Economic Geology*, 87, 620-649.

Goldhammer, R. K., Johnson, C. A., 2001, Middle Jurassic-Upper Cretaceous Paleogeographic evolution and sequence-stratigraphic framework of the northwest Gulf of México rim, *in*: Bartolini, C., Buffler, R. T., and Cantú-Chapa, A., (eds.), *The western Gulf of México Basin: Tectonics, sedimentary basins, and petroleum systems*: American Association of Petroleum Geologists Memoir 75, 45-81.

Gorton, M.P., Schandl, E.S., 2000, From continents to island arcs: A geochemical index of tectonic setting for arc-related and within-plate felsic to intermediate volcanic rocks: *Canadian Mineralogist*, 38, 1065-1073.

Goodfellow, W.D., Grapes, K., Cameron, B., Franklin, J.M., 1993, Hydrothermal alteration associated with massive sulfide deposits, Middle Valley, northern Juan de Fuca Ridge: *Canadian Mineralogist*, 31, 1025-1060.

Herrmann, W., Hill, A.P., 2001, The origin of chlorite-tremolite-carbonate rocks associated with the Thalanga VHMS deposit, north Queensland, Australia: *Economic Geology*, 96, 1149-1173.

Huston, D.L., 1993, The effect of alteration and metamorphism on wall rock to the Balcooma and Dry River South volcanic-hosted massive sulfide deposits, Queensland, Australia: *Journal of Geochemical Exploration*, 48, 277-307.

Huston, D.L., Large, R.R., 1987, Genetic and exploration significance of the zinc ratio, (100Zn/(Zn+Pb)) in massive sulfide systems: *Economic Geology*, 82, 1521-1539.

Iriondo, A., Kunk, M.J., Winick, J.A., CRM, 2003, ⁴⁰Ar/³⁹Ar Dating Studies of Minerals and Rocks in various areas in Mexico: USGS/CRM Scientific Collaboration (Part I), U.S. Department of the Interior, U.S. Geological Survey. Open-File Report 03-020 on-line edition.

Ishikawa, Y., Sawaguchi, T., Iwaya, S., Horiuchi, M., 1976, Delineation of prospecting targets for Kuroko deposits based on modes of volcanism of underlying dacite and alteration halos: *Mining Geology*, 26, 105-117 (in Japanese with English abstract).

Johnson, B.J., Montante-Martinez, J.A., Canela-Barboza, M., Danielson, T.J., 2000, Geology of the San Nicolás Deposit, Zacatecas, Mexico, *in* Sherlock, R.L. and Logan, M.A.V., eds., *VMS Deposits of Latin America*: Geological Association of Canada, Special Publication, 2, 71-85.

Khin, Z., Gemmell, J.B., Large, R.R., Mernagh, T.P., Ryan, C.G., 1996, Evolution and source of ore fluids in the stringer system, Hellyer VHMS deposit, Tasmania, Australia: Evidence from fluid inclusion microthermometry and geochemistry: *Ore Geology Review*, 10, 251-278.

Large, R.R., 1992, Australian volcanic-hosted massive sulfide deposits: Features, styles, and genetic models: *Economic Geology*, 87, 471-510.

Large, R.R., Gemmell, J.B., Paulick, H., Huston, D.L., 2001, The alteration boxplot: A simple approach to understanding the relationship between alteration mineralogy and lithogeochemistry associated with VHMS deposits: *Economic Geology*, 96, 957-971.

Larson, P.B., 1984, Geochemistry of the alteration pipe at the Bruce Cu-Zn volcanogenic massive sulfide deposit, Arizona: *Economic Geology*, 79, 1880-1896.

Lees, T., Zaw, K., Large, R.R., Huston, D.L., 1990, Rosebery and Hercules copper-lead-zinc deposits, *in* Hughes, F.E., ed., *Geology of the mineral deposits of Australia and Papua New Guinea*: Melbourne, Australasian Institute of Mining and Metallurgy, 1241-1247.

Lesher, C.M., Goodwin, A.M., Campbell, I.H., Gorton, M.P., 1986, Trace element geochemistry of ore-associated and barren felsic metavolcanic rocks in the Superior province, Canada: *Canadian Journal of Earth Sciences*, 23, 222-237.

López-Ramos, E., 1972, Estudio Geológico del Basamento ígneo y metamórfico de las Zonas Norte y Poza Rica: *Boletín de la Asociación Mexicana de Geólogos Petroleros*. (AMGP), Jul-Sep 1972, 266-323.

Lydon, J.W., 1988, Volcanogenic massive sulphide deposits, Part 1. A descriptive model: *Geoscience Canada Reprint Series*, 3, 145-154.

Lydon, J.W., 2010, Basinal dewatering via the basement: evidence for infiltration of Paleozoic basinal brines into Mesoproterozoic rocks of the Purcell anticlinorium, southeastern British Columbia: TGI-3 Workshop: Public Geoscience in Support of Base Metal Exploration, Cordilleran section: Geological Association of Canada, Vancouver, B.C., Programme and Abstracts, 67-70.

McGoldrick, P.J., Large, R.R., 1992, Geologic and geochemical controls on gold-rich stringer mineralization in the Que River deposit, Tasmania: *Economic Geology*, 87, 667-685.

Mortensen, J.K., Hall, B.V., Bissig, T., Friedman, R.M., Danielson, T., Olivier, J., Rhys, D.A., Ross, K.V., Gabites, J.E., 2008, Age and Paleotectonic setting of Volcanogenic Massive Sulfide Deposits in the Guerrero Terrane of Central Mexico: Constraints from U-Pb Age and Pb Isotope Studies: *Economic Geology*, 103, 117-140.

Morton, R.L., Franklin, J.M., 1987, Two-fold classification of Archean volcanic-associated massive sulfide deposits: *Economic Geology*, 82, 1057-1063.

Ohmoto, H., Skinner, B.J., 1983, The Kuroko and related volcanogenic massive sulfide deposits: *Economic Geology Monograph* 5, 604 pp.

Paulick, H., Herrmann, W., Gemmell, J.B., 2001, Alteration of felsic volcanics hosting the Thalanga massive sulfide deposit (Northern Queensland, Australia) and geochemical proximity indicators to ore: *Economic Geology*, 96, 1175-1200.

Pearce, J.A., Cann, J.R., 1973, Tectonic setting of basic volcanic rocks determined using trace element analysis: *Earth and Planetary Science Letters*, 19, 290-300.

Piercey, S.J., 2011, The setting, style, and role of magmatism in the formation of volcanogenic massive sulfide deposits: *Mineral Deposita*, 46, 449-471.

Pindell, J., 1985, Alleghenian Reconstruction and Subsequent Evolution of the Gulf of Mexico, Bahamas, and Proto-Caribbean: *Tectonics*, 4, 1-39.

Pindell, J., Maresch, W.V., Martens, U., Stanek, K., 2012, The Greater Antillean Arc: Early Cretaceous origin and proposed relationship to Central American subduction mélange: implications for models of Caribbean evolution: *International Geology Review*, 54, 131-143.

Riverin, G., Hodgson, C.J., 1980, Wall-rock alteration at the Millenbach Cu-Zn mine, Noranda, Quebec: *Economic Geology*, 75, 424-444.

Rueda-Gaxiola, J., 1998, El origen del Golfo de México y de sus subcuencas petroleras mexicanas, con base en la palinoestratigrafía de lechos rojos: *Revista Mexicana de Ciencias Geológicas*, 15(1), 78-86.

Rueda-Gaxiola, J., López-Ocampo, E., Dueñas, M.A., Rodríguez, J.L., Torres-Rivero, A., 1999, Palynostratigraphical method: Basis for defining stratigraphy and age of the Los San Pedro allogroup, Huizachal-Peregrina anticlinorium, Mexico: *Geological Society of America Special Paper*, 340, 229-269.

Sangster, D.F., 1972, Precambrian volcanogenic massive sulfide deposits in Canada. A review: *Canada Geological Survey Paper* 72-77, 44 p.

Schandl, E.S., Gorton, M.P., 2002, Application of high field strength elements to discriminate tectonic settings in VMS environments: *Economic Geology*, 97, 629-642.

Schardt, C., Cooke, D., Gemmell, J.B., Large, R.R., 2001, Geochemical Modeling of the Zoned Footwall Alteration Pipe, Hellyer Volcanic-Hosted Massive Sulfide Deposit, Western Tasmania, Australia: *Economic Geology*, 96, 1037-1054.

Schulz, K.J., 2012, Regional Environment: *in* Shanks, W.C.P. and Thurston, R. (eds., 2012), *Volcanogenic massive sulfide occurrence model: U.S. Geological Survey Scientific Investigations Report 2010-5070-C*, 345 pp.

Shikazono, N., Hoshino, M., Utada, M., Nakata, M., Ueda, A., 1998, Hydrothermal carbonates in altered wall rocks at the Uwamuki Kuroko deposits, Japan: *Mineralium Deposita*, 33, 346-358.

Shikazono, N., Ogawa, Y., Utada, M., Ishiyama, D., Mizuta, T., Ishikawa, N., Kubota, Y., 2008, Geochemical behavior of rare earth elements in hydrothermally altered rocks of the Kuroko mining area, Japan— *Journal of Geochemical Exploration*, 98(3) 65-79.

Shirozo, H., 1974, Clay minerals in altered wall rocks of the Kuroko-type deposits: *Society of Mining Geologists Japan Special Issue*, 6, 303-311.

Shriver, N.A., MacLean, W.H., 1993, Mass, volume and chemical changes in the alteration zone at the Norbec mine, Noranda, Quebec: Mineralium Deposita, 28, 157-166.

Sillitoe, R.H., 1982, Extensional habitats of rhyolite-hosted massive sulfide deposits: Geology, 10, 403-407.

Smirnov, V.I., 1944, Obrazovanie razlichnyx tipov gidrotermalnyx mestorozhdenii Tyan-Shanya v svyazi s evollyutsiei magmy: Sovetskaya Geologiya, 1.

Smirnov, V.I., 1963, Ocherki Metallogenii, in russian, Gosgeoltexizdat, 164 pp. (in russian).

Smirnov, V.I., 1968, Kolchedanie mestorozhdenia, in Genezis endoguenix rudnix mestorozhdenii, in russian, Moskva, Nedra, 586-647, (in russian).

Smirnov, V.I., 1976, Geologiya Poleznix Iskopaemix, (Geology of Mineral Deposits): Moskva, Nedra, 688 pp. (in russian).

Smirnov, V.I., Gorzhevskii, D.I., 1978, Mestorozhdenia svintsa i tsinka, in Rudnie mestorozhdenia SSSR, 2: Moskva, Nedra, p.168-246, (in russian).

Solomon, M. and Gaspar, O.C., 2001, Textures of the Hellyer Volcanic-Hosted Massive Sulfide Deposit, Tasmania—the Aging of a Sulfide Sediment on the Sea Floor: Economic Geology, 96, 1513-1534.

Starostin, V.I., 1979, Metody opredeleniya fiziko-mekanicheskix svoystv porod i rud pri rudno-petrofizicheskix issledovaniyakh, v knige laboratornye metody issledovaniya mineralov, rud i porod: Moskva, Izd. Moskovskogo Universiteta, 175-270, (in russian).

Starostin, V.I., 1984, Geodinamika i Petrofizika Rudnix Polei i Mestorozhdenii: Moskva, Nedra, p. 205, (in russian).

Starostin, V.I., Dergachev, A.L., 1982, Strukturno-petrofizicheskii analiz. v knige Geologo-strukturnye metody izucheniya endogenyx rudnyx mestorozhdenii: Moskva, 110 pp. (in russian).

Starostin, V.I., Dergachev, A.L., Seminskii, Zh. V., 2002, Strukturny Rudnyx polei i mestorozhdeniy: Moskva, Izd. Moskovskogo Universiteta, 352 pp., (in russian).

Trejo, P., 2001, Geology of the Fresnillo Southeast Mine, Zacatecas, Mexico, in Albinson, T., Nelson C.E. (eds), New Mines and Discoveries in Mexico and Central America: Society of Economic Geologists. Special Publication, 8, 105-113.

Vassallo, L.F., 1988a, Características de la composición mineralógica de las menas de la Veta Madre de Guanajuato, México: Revista Mexicana de Ciencias Geológicas, 7(2), 232-243.

Vassallo, L.F., 1988b, Metamorfismo de Contacto en la Porcion Sudoriental del Batolito Granítico de la Sierra de Guanajuato, Universidad Nacional Autónoma de México, Instituto de Geología, Tercer Simposio Geología Regional México, Memoria, 78-80.

Vassallo, L.F., 1995, Mineralogical study of F.I. Madero sedex deposit, Zacatecas-Mexico: Cia. M. Fresnillo, Internal report, 40pp.

Vassallo, L.F., 2003, Structural Control and Alteration of volcanics hosting the San Nicolás Massive Sulfide Deposit, Zacatecas, México: Vancouver, BC, Canada, GAC-MAC-SEG Vancouver-2003 Meeting, On The Edge Earth Science at North America's Western Margin, Abstracts, 28, 174-175, CD.

Vassallo, L.F., 2012, Geology and alteration of volcanics hosting the Jurassic San Nicolás VHMS deposit (southern Zacatecas, Mexico), Cordilleran GSA, Section - 108th Annual Meeting (29-31-March-2012), Paper No. 25-2, 44(3), 48 <http://gsa.confex.com/gsa/2012CD/finalprogram/abstract_201603.htm>.

Vassallo, L.F., Reyes-Salas, M., 2007, Selenian Polybasite from the Guanajuato Mining District, Mexico: Bol-e, Centro de Geociencias, Universidad Nacional Autónoma de México, 3(2), 1-16.

Vassallo, L.F., Solorio-Munguia, J.G., 2005, Regional structural control and alteration of volcanics hosting the San Nicolás massive sulfide deposit, Zacatecas, Mexico. GSA Annual meeting, SLC-2005, Salt Lake City, Utah, Paper No. 227-3, Abstracts with Programs, 37, 7, CD.

Vassallo, L.F., Olmos-Colunga, J., Villaseñor-Cabral, M.G., Girón-García, P., Lozano-Cobo, A., 1989, Alteraciones hidrotermales de las rocas encajonantes de la parte central de la Veta Madre de Guanajuato, Estado de Guanajuato - Características petrofísicas y químicas: Revista Mexicana de Ciencias Geológicas, 8(2), 211-222.

Vassallo, L.F., Starostin, V.I., Shatagin, N.N., 2000, Osnovnie cherti metalloguenii tsentralnoi Meksiki, (Fundamental Characteristics of the Metallogeny of the Central Part of Mexico). Izvestiya sektsii nauk o zemle (RAEN) Rossiiskoi Akademii Estestvennih Nauk: Journal Izvestiya Earth Sciences Section Russian Academy of Natural Sciences, Issue 5, 33-44b.

Vassallo, L.F., Sousa, J.E., Olalde, G., 2004, Time associated magmatism and mineralization at the central part of Mexico: St. Catharines 2004, GAC-MAC Joint Annual Meeting, St. Catharines, Ontario, Canada, Abstracts, 29, 385, CD.

Vassallo, L.F., Solorio, J.G., Ortega-Rivera, M.A., Sousa, J.E., Olalde, G., 2008, Paleogene magmatism and associated skarn-hydrothermal mineralization in the central part of Mexico: Bol-e, Centro de Geociencias, Universidad Nacional Autónoma de México, 4(3), 1-27.

Vélez, S. D., 1990, Modelo transcurrente en la evolución tectónico-sedimentaria de México: Boletín de la Asociación Mexicana de Geólogos Petroleros. (AMGP), XL(2), 1-35.

Winchester, J.A., Floyd, P.A., 1977, Geochemical discriminations of different magma series and their differentiation products using immobile elements: Chemical Geology, 20, 325-343.

Wood, D.A., 1980, The application of a Th-Hf-Ta diagram to problems of tectonomagmatic classification and to establishing the nature of crustal contamination of basaltic lavas of the British Tertiary volcanic province: Earth and Planetary Science Letters, 50, 11-30.

Yakovlev, G.F., 1959, Struktury rudnyx raionov, polei i mestorozhdenii Rudnogo Altaya. V sb.: Zakonomernosti razmesheniya poleznyx iskopaemyx, T.II, Izd. AN SSSR.

Zaw, K., Large, R.R., 1992, The precious metal-rich South Hercules mineralization, western Tasmania: A possible subseafloor replacement volcanic-hosted massive sulfide deposit: Economic Geology, 87, 931-952.

Manuscript received: August 6, 2014

Corrected manuscript received: April 13, 2015

Manuscript accepted: April 27, 2015